INTERNATIONAL JOURNAL FOR NUMERICAL METHODS IN FLUIDS
Int. J. Numer. Meth. Fluids 2007; **55**:737–783
Published online 24 April 2007 in Wiley InterScience (www.interscience.wiley.com). DOI: 10.1002/fld.1491

A modified conservation principles theory leading to an optimal Galerkin CFD algorithm

Sunil Sahu[1,‡] and A. J. Baker[2,*,†,§,¶]

[1]*CD-Adapco, Plymouth, MI 48170, U.S.A.*
[2]*CFD Laboratory, University of Tennessee, Knoxville, TN 37996, U.S.A.*

SUMMARY

A modified conservation principles theory in one, then multi-dimensions, admits the prediction of an optimally accurate algorithm construction for the unsteady incompressible Navier–Stokes (INS) equations. *Via* a time Taylor series (TS) operation, followed by a pseudo-limit process, the theory generates a modified, but still analytical, INS system parameterized by a set of coefficients constrained only by a convexity requirement. A spatially discretized finite element implementation of a Galerkin weak statement on this modified INS system, termed the 'Taylor weak statement (TWS),' generates a parameterized CFD algorithm for analysis. TWS algorithm phase velocity and amplification factor error functions are derived for linear and bilinear basis implementations assembled at the generic node. A subsequent TS expansion in wave number space admits analytical identification of parameter set options affecting lowest order error terms. The results of definitive verification- and validation-class computational experiments for a range of published CFD algorithms belonging to the TWS class, reported herein, clearly confirm theoretical prediction of the optimal TWS algorithm for INS thermal/fluid transport applications. Copyright © 2007 John Wiley & Sons, Ltd.

Received 9 March 2006; Revised 13 February 2007; Accepted 17 February 2007

KEY WORDS: CFD; error estimation; Fourier analysis; dispersion; numerical diffusion; optimization

1. INTRODUCTION

The comparative performance assessment of Navier–Stokes (NS) CFD algorithms, derived *via* a multitude of distinct theories, has occupied the imagination of analysts for decades. Fourier analysis

*Correspondence to: A. J. Baker, CFD Laboratory, University of Tennessee, Knoxville, TN 37996, U.S.A.
†E-mail: ajbaker@utk.edu
‡Senior Engineer.
§Professor, Engineering Science.
¶Director.

Contract/grant sponsor: NSF; contract/grant number: DUE 0121669
Contract/grant sponsor: ARC Automotive, Inc.

is the preferred theoretical framework supporting this activity, as it admits analytical determination, for linearizing assumptions, of phase velocity error and amplitude dissipation distributions across the wave number spectrum characterizing resolution on a mesh of measure h.

Chronologically, Belytschko and Mullen [1] pioneered a generalized Fourier analyses approach to assess consistent and lumped mass matrix forms on algorithm phase speed for linear and quadratic finite element (FE) formulations. Shortly thereafter, Vichnevetsky and Bowles [2], also Vichnevetsky [3], report the results for phase and group velocity distributions for hyperbolic statement algorithms implemented using both finite difference (FD) and FE methods. Shakib and Hughes [4] investigate the stability and accuracy of a space–time Galerkin Least Squares (GLS) method applied to advection–diffusion problems. Comparative phase and amplitude error analysis for FD schemes is reported by Morton and Mayers [5]. Christon [6] reports on FE mass matrix dispersive characteristics for a second-order wave equation. Most recently, Christon *et al*. [7, 8] develop a generalized Fourier analyses theory and a detailed procedure for estimation of error in phase and group speeds, discrete diffusivity and artificial diffusivity for 1D and 2D advection–diffusion problems.

The historical approach for generating a CFD algorithm has centred on forming spatially discrete approximations to the derivatives in the NS system, termed *a scheme* in the literature. All finite difference (FD) and finite volume (FV) CFD methods belong to this category. The alternative, purely analytical approach employs modern approximation theory, cf. Oden and Reddy [9], involving definition of a set of trial functions to support an NS system approximate solution, then forming a weak statement to render the approximation error (function) orthogonal to a defined set of test functions, Oden and Demkowicz [10]. The trial and test function spaces need only be sufficiently differentiable, hence square integrable, and the most common CFD algorithm implementation defines discrete subset spaces, called (FE) trial space bases, hence employs a domain meshing to implement the formulation. The available linear theory predicts the optimal algorithm, i.e. that exhibiting the *minimal error*, accrues to the trial and test spaces containing identical members, hence also their subsets, which generates a Galerkin weak statement (GWS) algorithm.

History has confirmed that a GWS algorithm for models of and genuine NS systems can indeed be optimally accurate as a function of completeness of the trial space bases. However, such an algorithm is well known to suffer from a dispersive error mechanism at large, i.e. practical, Reynolds number *Re*. This observation has led to derivation of a range of non-GWS CFD algorithms, each implemented with a test function set, explicitly modified to yield improved performance. The historical algorithms are due to Wahlbin [11], Dendy [12] and Raymond and Garder [13]. More recent developments are reported by Donea, [14], termed Taylor–Galerkin (TG), the well exercised Brooks–Hughes Streamline Upwind Petrov Galerkin (SUPG) formulation, [15], and GLS, cf. Jiang [16].

These non-Galerkin CFD algorithms each result from an apparently quite distinct theoretical foundation. As a first step in the search for an analytical formulation process, Donea interchanged the traditional spatial–temporal discretization sequence, hence produced the time-explicit TG algorithm. This operation produced a non-Galerkin appearing test function within a GWS. Baker and Kim [17] generalized the theoretical approach, *via* an approximate limiting process, resulting in an *analytical restatement* of the parent NS system, eligible for a genuine GWS construction for implementation *via any* space–time discretization process. The key development contribution was direct embedding of a coefficient set $\{\alpha, \beta, \gamma, \mu, \theta\}$ in the *continuum* TS-modified NS system, theoretically constrained only by a convexity requirement.

DOI: 10.1002/fld

Table I. TWS formulation categorization of independently derived CFD algorithms.

Algorithm name	θ	α	β	γ	μ
$\text{TWS}^h + \theta\text{TS}$	All	Arbitrary	Arbitrary	Arbitrary	Arbitrary
(Bubnov) Galerkin	All	0	0	0	0
Donor cell FD	0	0	u/C	$1/C^2$	0
Lax–Wendroff FD	0	0	$\text{sgn}(u)$	0	0
Taylor Galerkin (TG)	0	0	1	1	0
Crank–Nicolson TG	0.5	0	0.5	1	0
Euler Char. Galerkin	0	0	1	0	1
Swansea TG	0	0	1	0	0
Wahlbin	0	$\text{sgn}(u)$	$2\,\text{sgn}(u)$	0	0
Dendy	0	$h\,\text{sgn}(u)$	$h\,\text{sgn}(u)$	0	0
Raymond–Garder	0.5	$2v_0\,\text{sgn}(u)/C$	$2v_0\,\text{sgn}(u)/C$	0	0
Hughes SUPG (steady)	—	0	$\text{sgn}(u)$	0	0
Euler Petrov Galerkin	0	0	0	$(1-v)$	0
CN Petrov Galerkin	0.5	$\text{sgn}(u)$	$v\,\text{sgn}(u)$	$-v/2$	0
Warming–Beam FD	0	0	1	0	$-3(1-C)$
van Leer MUSCL	1	0	$\text{sgn}(u)$	0	-3
Galerkin least squares	All	2θ	2θ	0	0

Note: $\text{sgn}(u)$ is the sign of u, $v_0 = 1/\sqrt{15}$, $C \leqslant v \leqslant 1$, C is the Courant number.

A GWS written on the TS-modified NS system, when implemented using the FE linear basis in 1D, and an implicit time discretization, led to the Taylor weak statement (TWS) modified hyperbolic conservation law algorithm, [17]. Being a genuine Galerkin formulation, the error associated with any approximate solution to the TS-modified conservation principle is rendered orthogonal to the approximation trial space, hence should exhibit optimal accuracy. Of theoretical significance, it was also observed that the TWS formulation admitted recovery of well over a dozen independently derived CFD algorithms, upon interpretation of appropriate definitions for the TWS parameter set $\{\alpha, \beta, \gamma, \mu, \theta\}$. Table I summarizes this published observation for the 1D, unsteady scalar advection–diffusion problem.

The extension of the TWS theory to semi-discrete implementation with FE quadratic and cubic bases in 1D, as well as spectral error distribution comparisons to the FD and FV algorithm constructions popular with incompressible Navier–Stokes (INS) CFD codes, is reported by Chaffin and Baker [18]. The key results generated were: (1) identification of 'optimal-γ' TWS formulations for the pure advection problem, with γ dependent on FE trial space basis completeness degree b; and (2) spectral characterization of the dissipative nature of the TWS theory β term. Reported results confirmed the optimal-γ TWS algorithm matched the pure GWS algorithm performance, in wave number space, for implementation using one-degree lower b FE bases, resulting in significant economy based on matrix band width of these formulations.

Continuing with this study, Kolesnikov and Baker [19] derive the TWS modified conservation principle CFD algorithm for the steady INS system. A premier contribution was theory generation, in the *continuum* and in multi-dimensions, of the identical velocity tensor product coefficient associated with the β term in the unsteady TWS theory. The steady INS theory removed the arbitrariness of the unsteady TWS β coefficient, analytically replacing it with $h^2 Re/12$ in the limit of large Reynolds number Re, for h a measure of the FE bilinear basis mesh in 2D and 3D. Additionally, the steady theory predicted a TWS solution asymptotic convergence rate to be order

DOI: 10.1002/fld

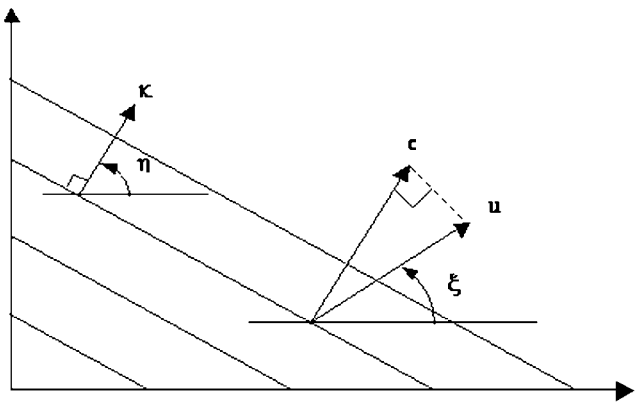

Figure 1. Wave number vector and phase velocity in the Cartesian continuum.

h^4, in an energy semi-norm, for a FE bilinear basis implementation. This matches the convergence rate of a FE quadratic basis GWS implementation, and computational results for verification- and benchmark-class INS problem statements fully verified these theoretical predictions.

The goal therefore is to complete the theoretical assessment of the published range of TWS-type CFD algorithms, including extension to multi-dimensions. Recalling Table I, algorithms belonging to the class but not yet characterized in the TWS context include SUPG, TG, GLS and the earlier algorithms of the Raymond–Garder (RG), Wahlbin, and Dendy class. The newly developed class of weak statement algorithms named 'Discontinuous Galerkin (DG)' methods, cf. Li [20] do not readily fit the TWS analysis framework, as they require selection of a *scheme* for interface flux evaluations, a key formulation ingredient of FV and/or flux splitting CFD methods.

Completing the goal requires generation of the class of TWS algorithm solutions in wave number space. For a mesh of measure h supporting a space-discrete implementation, resolution hence propagation of solution spectral content of scale order $2h$ is substantially (totally) compromised. This results in the cascading of solution order $2h$ spectral content into longer wavelength spurious oscillations termed *dispersion error*. Artificial (numerical) diffusion mechanisms can stabilize a computation, but at the same time generate algorithm *dissipation error*. The phase velocity $\mathbf{c}$ is the velocity of propagation of a solution component (called a 'wave') of velocity $\mathbf{u}$ in the direction of the wave number vector $\boldsymbol{\kappa}$ [21] Figure 1. Mathematically,

$$\mathbf{c} = \frac{(\mathbf{u} \cdot \boldsymbol{\kappa})\boldsymbol{\kappa}}{\kappa^2} \tag{1}$$

where $\kappa \equiv |\boldsymbol{\kappa}|$ is the wave number, i.e. the number of wave crests existing in the interval 2π in the direction of the wave vector angle η [22]. Thereby, $\kappa = 2\pi/\lambda$, where λ is the crest wavelength and $\boldsymbol{\kappa}$ is orthogonal to the wave crest. In 1D, the phase velocity (speed) is the scalar c, identical with the imposed speed u. The group velocity $\mathbf{V_g}(\boldsymbol{\kappa})$ is the velocity with which smooth waves propagate energy in a dispersive medium. In 2D and rectangular Cartesian coordinates

$$\mathbf{V_g}(\boldsymbol{\kappa}) = \nabla_\kappa \omega = \begin{bmatrix} \dfrac{\partial \omega}{\partial \kappa_1}\hat{\mathbf{i}} \\ \dfrac{\partial \omega}{\partial \kappa_2}\hat{\mathbf{j}} \end{bmatrix} \tag{2}$$

DOI: 10.1002/fld

where ω is cyclic frequency and $\kappa_1 = \kappa \cos\eta$, thereby $\kappa_2 = \kappa \sin\eta$, is the wave number resolution in the x and y directions, respectively. In the continuum, group velocity is independent of $\boldsymbol{\kappa}$ and is equal to the imposed velocity.

For a spatially discrete algorithm implementation, the phase and group velocities differ from their continuum values due to discretization-induced wave number dependence. Further, the group velocity is not always aligned with the wave vector but instead has a propagation direction φ defined by

$$\varphi = \tan^{-1}\left(\frac{V_{g,y}}{V_{g,x}}\right) = \tan^{-1}\left(\frac{\partial\omega/\partial\kappa_1}{\partial\omega/\partial\kappa_2}\right) \tag{3}$$

Reverting to 1D, from (1)–(3)

$$V_g(\kappa) = \frac{\partial\omega(\kappa)}{\partial\kappa} = \frac{\partial(c(\kappa)\kappa)}{\partial\kappa} = c(\kappa) + \kappa\frac{\partial(c(\kappa))}{\partial\kappa} \tag{4}$$

hence only if phase speed c is independent of wave number κ are the group and phase speeds equal. Therefore, determination of the wave number dependence of phase speed, hence phase velocity in one- and multi-dimension is the key theoretical assessment.

This paper presents complete theoretical characterization of the class of TWS CFD algorithms for the INS system. *Via* Fourier analysis, the theory for the TWS arbitrary coefficient set $\{\alpha, \beta, \gamma, \theta\}$ becomes ultimately expressed as a Taylor series (TS) cast in non-dimensional wave number space. The theory is completed in one and two space dimensions, hence extension to 3D inferred. The *optimal* linear and bilinear FE basis TWS algorithms thus become identified in all dimensionalities, for the restriction of uniform discretizations in rectangular cartesian coordinates.

Numerical results are reported for non-diffusive verification-class problem statements which fully validate the theory. Additionally, in 2D, results quantify the loss of optimal TWS algorithm accuracy when implemented on an unstructured mesh spanned by the linear natural coordinate FE basis on triangles. Finally, GWS and optimal-γ TWS algorithm solutions are compared, for a genuine INS fluid-thermal 2D validation problem, providing solid quantification of the developed theory accuracy.

2. MODIFIED CONSERVATION PRINCIPLES FORMULATION

2.1. Problem statement

The unsteady, INS conservation principles for mass, momentum and energy in non-dimensional tensor index form are familiarly

$$\text{DM:} \quad \mathscr{L}(\rho_0) = \frac{\partial u_i}{\partial x_i} = 0 \tag{5}$$

$$\text{DP:} \quad \mathscr{L}(u_i) = \frac{\partial u_i}{\partial t} + \frac{\partial}{\partial x_j}\left(u_i u_j + P\delta_{ij} - Re^{-1}\frac{\partial u_i}{\partial x_j}\right) + \frac{Gr}{Re^2}\Theta\hat{g}_i = 0 \tag{6}$$

$$\text{DE:} \quad \mathscr{L}(\Theta) = \frac{\partial\Theta}{\partial t} + u_i\frac{\partial\Theta}{\partial x_i} - \frac{1}{Re\,Pr}\frac{\partial^2\Theta}{\partial x_i^2} - s = 0 \tag{7}$$

DOI: 10.1002/fld

In (5)–(7), u_i is the velocity vector, $P = p/\rho_0$ is the kinematic pressure for ρ_0 the constant density, Θ is the potential temperature and s is a heat source. The non-dimensional groups parameterizing solutions to (5)–(7) are

$$\text{Grashoff number:} \quad Gr = \frac{g\tau\Delta T L^3}{\nu^2} \tag{8}$$

$$\text{Reynolds number:} \quad Re = \frac{UL}{\nu} \tag{9}$$

$$\text{Prandtl number:} \quad Pr = \frac{\rho_0 \nu c_p}{k} \tag{10}$$

where τ is the thermal expansion coefficient associated with the Boussinesq buoyancy approximation, [23], ν is kinematic viscosity, c_p is the heat capacity at constant pressure and k is thermal conductivity. The PDE system (6)–(10) constitutes an initial-value, elliptic boundary value (EBV) problem statement, for finite *Re*, with solution process subject to the DM differential constraint (5).

2.2. *Modified conservation principles parameterization*

TWS formation, followed by the approximate limiting of the TS modified conservation principles construction, is fully detailed in [17]. The resultant TS-modified INS statement for DP embeds the arbitrary parameter set $\{\alpha, \beta, \gamma, \mu\}$ as

$$\begin{aligned}\mathscr{L}^m(u_i) = \mathscr{L}(u_i) &- \frac{\Delta t}{2}\frac{\partial}{\partial x_j}\left(\alpha u_j \frac{\partial u_i}{\partial t} + \beta u_j u_k \frac{\partial u_i}{\partial x_k}\right) \\ &- \frac{\Delta t^2}{6}\frac{\partial}{\partial x_j}\left[\gamma u_j u_k \frac{\partial}{\partial x_k}\frac{\partial u_i}{\partial t} + \mu u_j u_k \frac{\partial}{\partial x_k}\left(u_m \frac{\partial u_i}{\partial x_m}\right)\right] + O(\Delta t^3) = 0\end{aligned} \tag{11}$$

where $\mathscr{L}(u_i)$ in (11) remains (6) in completeness. Non-linearities in (11) severely limit theoretical analysis, which is not the case for scalar field transport, e.g. (7). The corresponding TS-modified conservation principle for any scalar field $q(x_j, t)$ is

$$\begin{aligned}\mathscr{L}^m(q) = \mathscr{L}(q) &- \frac{\Delta t}{2}\frac{\partial}{\partial x_j}\left(\alpha u_j \frac{\partial q}{\partial t} + \beta u_j u_k \frac{\partial q}{\partial x_k}\right) \\ &- \frac{\Delta t^2}{6}\frac{\partial}{\partial x_j}\left[\gamma u_j u_k \frac{\partial}{\partial x_k}\frac{\partial q}{\partial t} + \mu u_j u_k \frac{\partial}{\partial x_k}\left(u_m \frac{\partial q}{\partial x_m}\right)\right] + O(\Delta t^3) = 0\end{aligned} \tag{12}$$

which is amenable to the exacting theoretical analysis detailed in the following.

3. THEORETICAL DEVELOPMENT

3.1. *TWS algorithm formulation for INS*

Via the classical weak statement process, Baker [24], any approximation solution q^N to (11) and (12) is defined as an inner product of a set of trial space functions $\Psi_\chi(\mathbf{x})$ with a set of

DOI: 10.1002/fld

time-dependent expansion coefficients, specifically

$$q(\mathbf{x}, t) \approx q^N(\mathbf{x}, t) = \sum_{\chi}^{N} \Psi_\chi(\mathbf{x})\, Q_\chi(t) \tag{13}$$

The associated approximation error is the function $e^N(\mathbf{x}, t) \equiv q(\mathbf{x}, t) - q^N(\mathbf{x}, t)$ distributed on the domain of definition of the INS problem statement. This function is mathematically extremized, which in practice becomes minimization, by rendering it orthogonal to the space of trial functions $\Psi_\chi(\mathbf{x})$. This defines the GWS criterion (identical trial and test spaces), hence the GWS for the Taylor-modified INS system approximate solution (13) is

$$\mathrm{TWS}^N \equiv \int_\Omega \Psi_\zeta \mathscr{L}^m(q^N)\, \mathrm{d}\tau \equiv \{0\} \quad \text{for all } \zeta \tag{14}$$

Assuming the integrals defined in (14) can be evaluated, all $\mathbf{x}$-dependence vanishes yielding a large system of ordinary differential equations of the form

$$\mathrm{TWS}^N = [\mathrm{MASS}(\alpha, \gamma)]\frac{\mathrm{d}\{Q\}}{\mathrm{d}t} + \{\mathrm{RES}\} = \{0\} \tag{15}$$

where [MASS] is the TWS $\{\alpha, \gamma\}$-term augmented 'mass matrix' and RES contains all other contributions from (14), including the TWS $\{\beta, \mu\}$-terms. The single-stage Euler TS in time with implicitness parameter θ is

$$\theta\mathrm{TS}:\ \{Q\}_{n+1} = \{Q\}_n + \Delta t(\theta\{Q\}'_{n+1} + (1-\theta)\{Q\}'_n) + O(\Delta t^{f(\theta)}) \tag{16}$$

Equation (15) defines the time derivative as $\mathrm{d}\{Q\}/\mathrm{d}t = \{Q\}' = -[\mathrm{MASS}]^{-1}\{\mathrm{RES}\}$, hence substituting into (16) and multiplying through by [MASS] produces the computable algebraic statement

$$\mathrm{TWS}^N + \theta\mathrm{TS} \Rightarrow [\mathrm{JAC}(\alpha, \beta, \gamma, \mu, \theta, \{Q\})]\{\delta Q\}^{p+1} = -\{\mathrm{F}Q(\{Q\}, \alpha, \beta, \gamma, \mu, \theta, p)\} \tag{17}$$

$$\{\mathrm{F}Q\} = [\mathrm{MASS}(\alpha, \gamma)]\{\Delta Q\} + \{\mathrm{RES}(\{Q\}_{n+\theta}, \beta, \mu)\} \tag{18}$$

In (17), p is the matrix iteration index with $\{\delta Q\}$ the state variable current iterate. Further in (18), $\{\Delta Q\} \equiv \{Q\}_{n+1} - \{Q\}_n$ for $\{Q\}_{n+1}$ the estimate for the current solution, where n, $n+1$ denote time stations. The solution essence is

$$\{\delta Q\}^{p+1} = -[\mathrm{JAC}(\alpha, \beta, \gamma, \mu, \theta, \{Q\})]^{-1}\{FQ(\{Q\}, \alpha, \beta, \gamma, \mu, \theta, p)\} \tag{19}$$

where $[\mathrm{JAC}] \equiv \partial\{FQ\}/\partial\{Q\}$ is the TWS algorithm jacobian matrix, and the indicated matrix inverse is replaced by a Krylov-type solver.

3.2. TWS algorithm FE discrete implementation

The $\mathrm{TWS}^N + \theta\mathrm{TS}$ weak statement theory for the INS system is complete. What remains is to convert (14)–(18) into computable form, hence also enforce the constraint of continuity (5). The standard approach is to define the approximate solution $q^N(\mathbf{x}, t)$ in a spatially discrete form, herein denoted $q^h(\mathbf{x}, t)$, where h denotes a measure of the computational mesh. The implementation devoid of any heurism is to project the spatially discrete approximation onto the union of FE

DOI: 10.1002/fld

trial space basis functions $\{N_b(\mathbf{x})\}$ constituted of polynomials complete to degree b. The formal statement is

$$q(\mathbf{x}, t) \approx q^N(\mathbf{x}, t) \equiv q^h(\mathbf{x}, t) = \bigcup_e q_e(\mathbf{x}, t) = \bigcup_e \{N_b(\mathbf{x})\}^{\mathrm{T}} \{Q(t)\}_e \tag{20}$$

and (17) and (18) become analytically evaluated, *via* the formal calculus without arbitrariness, i.e. no *scheme* is involved.

With the FE discrete implementation decision, the available asymptotic convergence theory [9] predicts that for $Re^{-1} > 0$, i.e. viscosity effects are non-vanishing, the associated semi-discrete approximate solution error is bounded as

$$\|e^h(n\Delta t)\|_E \leqslant C_{\mathbf{x}} h_e^{2\xi} \|\text{data}\|_{\Omega, \partial\Omega} + C_t \Delta t^{f(\theta)} \|Q(t_0)\|_{\Omega \cup \partial\Omega}, \quad \xi = \min(b, r-1) \tag{21}$$

In (21) the constants C_ω are independent of h and Δt, respectively, the measure of the computational mesh Ω^h and the time step interval, and $\|\cdot\|$ denotes a suitable norm, cf. Baker [24]. Thereby, convergence is controlled by b, the completeness degree of the FE basis, unless compromised by r, a smoothness measure of the exact solution, hence all *data* driving the solution. In the alternative instance of viscous effects being negligible, i.e. $Re^{-1} \Rightarrow 0$, the mesh measure exponent in (21) degenerates to $\xi = \min(1, r-1)$, hence the asymptotic convergence rate is independent of FE basis completeness degree b.

3.3. Fourier representation in 1D

The TS-modified scalar transport equation (12) simplified to 1D is

$$\begin{aligned} \mathscr{L}^m(q) = {} & \frac{\partial q}{\partial t} + u\frac{\partial q}{\partial x} - \frac{1}{Pa}\frac{\partial^2 q}{\partial x^2} - \frac{\Delta t}{2}\frac{\partial}{\partial x}\left(\alpha u \frac{\partial q}{\partial t} + \beta u^2 \frac{\partial q}{\partial x}\right) \\ & - \frac{\Delta t^2}{6}\frac{\partial}{\partial x}\left[\gamma u^2 \frac{\partial}{\partial x}\frac{\partial q}{\partial t} + \mu u^2 \frac{\partial}{\partial x}\left(u\frac{\partial q}{\partial x}\right)\right] + O(\Delta t^3) = 0 \end{aligned} \tag{22}$$

where Pa is the placeholder for the non-D parameter appropriate to q. For example, in (7) $Pa = Re\,Pr$, while for mass transport $Pa = ReSc$, where Sc is the Schmidt number associated with binary diffusion.

The amplification factor G^h associated with the discrete approximate solution $q^h(x,t)$ is determined by assembling $\mathrm{TWS}^h + \theta\mathrm{TS}$, (17), for (20) at the generic mesh node X_j. The resultant recursion stencil for the linear ($b = 1$) FE basis implementation is

$$\boxed{a_{j-1}\, a_j\, a_{j+1}} \begin{bmatrix} Q_{j-1}^{n+1} \\ Q_j^{n+1} \\ Q_{j+1}^{n+1} \end{bmatrix} = \boxed{b_{j-1}\, b_j\, b_{j+1}} \begin{bmatrix} Q_{j-1}^{n} \\ Q_j^{n} \\ Q_{j+1}^{n} \end{bmatrix} \tag{23}$$

where $Q_{j-1,j,j+1}$ are nodal values of the approximate solution and the coefficients a_j and b_j contain all mesh-generated constants, INS parameters, and the TWS parameter set, recall (17), omitting the μ term since the $b = 1$ basis will not support the required differentiability. Recalling

DOI: 10.1002/fld

the Fourier representations

$$Q_{j-1} = Q(x - \Delta x) = Q_j \mathrm{e}^{-\mathrm{i}m} \tag{24}$$

$$Q_{j+1} = Q(x + \Delta x) = Q_j \mathrm{e}^{+\mathrm{i}m} \tag{25}$$

and substituting into (23), the solution for the TWS algorithm amplification factor is

$$G^h = \frac{b_{j-1}\mathrm{e}^{-\mathrm{i}m} + b_j + b_{j+1}\mathrm{e}^{\mathrm{i}m}}{a_{j-1}\mathrm{e}^{-\mathrm{i}m} + a_j + a_{j+1}\mathrm{e}^{\mathrm{i}m}} \tag{26}$$

Inserting data pertinent to the linear FE basis implementation of (17) yields (26) as the rational polynomial of complex arguments

$$G^h_{\mathrm{FE}(k=1)} = \frac{(2+\gamma C^2 - 3(1-\theta)\beta C^2 - 6(1-\theta)D) + (1-\gamma C^2 + 3(1-\theta)\beta C^2 + 6(1-\theta)D)\cos m - \mathrm{i}3C(\frac{1}{2}\alpha + (1-\theta))\sin m}{(2+\gamma C^2 + 3\theta\beta C^2 + 6D\theta) + (1-\gamma C^2 - 3\theta\beta C^2 - 6D\theta)\cos m - \mathrm{i}3C(\frac{1}{2}\alpha - \theta)\sin m} \tag{27}$$

In (27), $m = \kappa h$ is the non-dimensional wave number, h is the measure of the (assumed) uniform mesh, $C = U\Delta t/h$ is the Courant number, equivalent to the non-dimensional time step, and $D \equiv \Delta t/Pah^2$ is the placeholder for the action of physical diffusion.

Any TWS$^h + \theta$TS algorithm will exhibit discrete approximation error e^h, as a function of wave number m dependent upon the parameter set choice. For stability, the amplification factor (27) magnitude must be bounded as $|G^h| \leqslant 1$. Any TWS$^h + \theta$TS algorithm m-dependent relative phase velocity is computable from the real and imaginary components of the amplification factor (27) as

$$\Phi^h = \frac{1}{-mC}\tan^{-1}\left(\frac{\mathrm{Imag}(G^h)}{\mathrm{Real}(G^h)}\right) \tag{28}$$

A precise statement of algorithm discrete approximation error in wave number space accrues to multiplying (27) through by the complex conjugate, then clearing the denominator *via* a TS operation of sufficiently high order. The solution remains a complex function and the resultant TS to order seven in m is presented as Equation (29).

$$G^h_{\mathrm{FE}(k=1)} = 1 - \mathrm{i}Cm + \left[\frac{1}{2}(\alpha - \beta - D) - \theta\right]C^2m^2 + \mathrm{i}\left[\begin{array}{l}\left(\frac{1}{4}\alpha(\alpha-\beta) + \frac{\gamma}{6} + (-\alpha+\beta)\theta + \theta^2\right)C^3 \\ \quad + CD\left(-\frac{\alpha}{2} + 2\theta\right)\end{array}\right]m^3$$

$$+ C^2\left[\begin{array}{l}-\frac{\beta}{24} + C^2\left(\frac{\alpha^2}{8}(-\alpha+\beta) + \frac{\gamma}{6}\left(-\alpha + \frac{\beta}{2}\right) + \left(\alpha\left(\frac{3}{4}\alpha - \beta\right) + \frac{1}{4}\beta^2 + \frac{1}{3}\gamma\right)\theta\right. \\ \quad \left. + \frac{3}{2}(-\alpha+\beta)\theta^2 + \theta^3\right)D\left(\frac{-1}{12C^2} + \frac{\theta D}{C^2} + \left(\frac{\alpha^2}{4} + \frac{\gamma}{6} - 2\alpha\theta + \beta\theta + 3\theta^2\right)\right)\end{array}\right]m^4$$

DOI: 10.1002/fld

$$
\begin{aligned}
&+\mathrm{i}C\left[\begin{array}{l}
\dfrac{1}{180}+C^2\left(\dfrac{-\alpha\beta}{48}+\dfrac{\gamma}{72}+\dfrac{\beta\theta}{12}\right)+C^4\left\{\dfrac{-\alpha^3}{16}(\alpha-\beta)-\dfrac{\alpha\gamma}{4}\left(\dfrac{\alpha}{2}-\dfrac{\beta}{3}\right)-\dfrac{\gamma^2}{36}\right\}\\
\quad+C^4\left\{\theta\left(\dfrac{\alpha^3}{2}-\dfrac{\alpha\beta}{4}(3\alpha-\beta)+\gamma\left(\dfrac{\alpha}{2}-\dfrac{\beta}{3}\right)\right)\right\}\\
\quad+C^4\theta^2\left\{\dfrac{-3\alpha}{2}\left(\alpha-\dfrac{3\beta}{2}\right)-\dfrac{3\beta^2}{4}-\dfrac{\gamma}{2}\right\}\\
\quad+C^4(2\theta^3(\alpha-\beta)-\theta^4)+D\left(\dfrac{-\alpha}{24}+\dfrac{\theta}{6}+(\alpha-3\theta)\theta D\right.\\
\quad\left.+C^2\left(\dfrac{\alpha^3}{8}+\dfrac{\alpha\gamma}{6}+\left(-\dfrac{3}{2}\alpha+\beta\right)\alpha\theta-\dfrac{2}{3}\gamma\theta+\left(\dfrac{9}{2}\alpha-3\beta-4\theta\right)\theta^2\right)\right)
\end{array}\right]m^5\\
&+C^2\left[\begin{array}{l}
\dfrac{-\alpha}{180}-\dfrac{\beta}{720}+\dfrac{\theta}{90}+C^2\left\{\dfrac{\alpha\beta}{12}\left(\dfrac{\alpha}{8}-\theta\right)-\dfrac{\gamma}{72}(\alpha-\beta)+\dfrac{\gamma\theta}{36}+\dfrac{\beta\theta}{8}\left(\dfrac{\beta}{3}+\theta\right)\right\}\\
\quad+C^4\left\{\dfrac{\alpha^5}{32}-\dfrac{\alpha^4\beta}{32}+\dfrac{\alpha^2\gamma}{4}\left(\dfrac{\alpha}{3}-\dfrac{\beta}{4}\right)+\dfrac{\gamma^2}{24}\left(\alpha-\dfrac{\beta}{3}\right)\right\}\\
\quad+C^4\theta\left\{\dfrac{-5\alpha^4}{16}+\dfrac{\alpha^2\beta}{2}\left(\alpha-\dfrac{3\beta}{16}\right)+\dfrac{\gamma}{2}\left(-\alpha(\alpha-\beta)-\dfrac{1}{6}(\beta^2+\gamma)\right)\right\}\\
\quad+\theta^2C^4\left\{\dfrac{5\alpha^3}{4}+9\alpha\beta\left(-\dfrac{\alpha}{4}+\dfrac{\beta}{8}\right)-\dfrac{\beta^3}{8}+\gamma\left(\alpha-\dfrac{3\beta}{4}\right)\right\}\\
\quad+C^4\theta^3\left\{\dfrac{-1}{2}\left(5\alpha^2+3\beta^2\right)+4\alpha\beta-\dfrac{2}{3}\gamma+\dfrac{5}{2}\theta\,(\alpha-\beta)\right\}-C^4\theta^5\\
\quad+D\left(\dfrac{1}{C^2}\left(\dfrac{-1}{360}+\dfrac{1}{6}D\theta-D^2\theta^2\right)+\dfrac{\alpha^2}{48}+\dfrac{\gamma}{36}-\dfrac{1}{6}\alpha\theta-\dfrac{3}{4}D\alpha^2\theta\right.\\
\quad\left.+\dfrac{1}{6}\beta\theta-\dfrac{1}{3}D\gamma\theta+\dfrac{\theta^2}{4}+\dfrac{9}{2}D\alpha\theta^2-\dfrac{3}{2}D\beta\theta^2-6D\theta^3\right)
\end{array}\right]m^6\\
&+C^2\left[DC^2\left(-\dfrac{\alpha^4}{16}-\dfrac{1}{8}\alpha^2\gamma-\dfrac{\gamma^2}{36}+\alpha^3\theta-\dfrac{3}{4}\alpha^2\beta\theta+\alpha\gamma\theta-\dfrac{1}{3}\beta\gamma\theta-\dfrac{9}{2}\alpha^2\theta^2\right.\right.\\
&\left.\left.\quad+\dfrac{9}{2}\alpha\beta\theta^2-\dfrac{3}{4}\beta^2\theta^2-\dfrac{3}{2}\gamma\theta^2+8\alpha\theta^3-6\beta\theta^3-5\theta^4\right)\right]m^6\\
&+O(m^7)
\end{aligned}
\tag{29}
$$

Finally, the analytical expression for TWS approximation error requires knowledge of the exact solution, which for a 1D advection–diffusion problem is

$$q(x,t)=\exp[\mathrm{i}\kappa(x-ut)-\kappa^2Dt] \tag{30}$$

DOI: 10.1002/fld

The corresponding amplification factor is the ratio of solutions at two successive times computed at location x:

$$G_{\text{exact}} = \frac{q(x,(n+1)t)}{q(x,nt)} = \exp(-\mathrm{i}Cm - Dm^2) \tag{31}$$

and the associated TS is

$$G_{\text{exact}} = 1 - \mathrm{i}Cm - \left(\frac{C^2}{2} + D\right)m^2 + \mathrm{i}C\left(\frac{C^2}{6} + D\right)m^3 + \left[C^2\left(\frac{C^2}{24} + \frac{D}{2}\right) + \frac{D^2}{2}\right]m^4$$
$$- \mathrm{i}C\left(\frac{C^4}{120} + \frac{DC^2}{6} + \frac{D^2}{2}\right)m^5 - \left[C^2\left(\frac{C^4}{720} + \frac{C^2D}{24} + \frac{D^2}{4}\right) + \frac{D^3}{6}\right]m^6 + O(m^7) \tag{32}$$

The phase velocity (speed) error in a TWS^h + θTS algorithm is $c^h \equiv G_{\text{exact}} - G^h$, approximated as the difference between the TS expansions (29) and (32). Discarding the D terms, since the focus is on the action of the parameter set $\{\alpha, \beta, \gamma, \theta, C\}$ in the absence of physical diffusion, the phase error for $b = 1$ FE basis implementation, to the seventh order in wave number m, is

$$c^h_{\text{FE}(k=1)} = -[1 + 2\theta + (\alpha - \beta)]\frac{C^2m^2}{2} + \mathrm{i}\left[\frac{1}{6} - \frac{1}{4}\alpha(\alpha - \beta) - \frac{\gamma}{6} - (-\alpha + \beta)\theta - \theta^2\right]C^3m^3$$
$$+ C^2\left[\frac{C^2}{24} + \frac{\beta}{24} - C^2\left(\frac{\alpha^2}{8}(-\alpha + \beta) + \frac{\gamma}{6}\left(-\alpha + \frac{\beta}{2}\right)\right.\right.$$
$$\left.\left. + \left(\alpha\left(\frac{3}{4}\alpha - \beta\right) + \frac{1}{4}\beta^2 + \frac{1}{3}\gamma\right)\theta + \frac{3}{2}(-\alpha + \beta)\theta^2 + \theta^3\right)\right]m^4$$
$$+ \mathrm{i}C\left[\begin{array}{l} -\dfrac{C^4}{120} - \dfrac{1}{180} - C^2\left(\dfrac{-\alpha\beta}{48} + \dfrac{\gamma}{72} + \dfrac{\beta\theta}{12}\right) \\ \quad - C^4\left\{\dfrac{-\alpha^3}{16}(\alpha - \beta) - \dfrac{\alpha\gamma}{4}\left(\dfrac{\alpha}{2} - \dfrac{\beta}{3}\right) - \dfrac{\gamma^2}{36}\right\} \\ \quad - C^4\left\{\theta\left(\dfrac{\alpha^3}{2} - \dfrac{\alpha\beta}{4}(3\alpha - \beta) + \gamma\left(\dfrac{\alpha}{2} - \dfrac{\beta}{3}\right)\right)\right\} \\ \quad - C^4\theta^2\left\{\dfrac{-3\alpha}{2}\left(\alpha - \dfrac{3\beta}{2}\right) - \dfrac{3\beta^2}{4} - \dfrac{\gamma}{2}\right\} \\ \quad - C^4(2\theta^3(\alpha - \beta) - \theta^4) \end{array}\right]m^5$$

DOI: 10.1002/fld

$$+C^2\left[\begin{array}{l}
-\dfrac{C^4}{720}+\dfrac{\alpha}{180}+\dfrac{\beta}{720}-\dfrac{\theta}{90}-C^2\left\{\dfrac{\alpha\beta}{12}\left(\dfrac{\alpha}{8}-\theta\right)\right.\\
\left.-\dfrac{\gamma}{72}(\alpha-\beta)+\dfrac{\gamma\theta}{36}+\dfrac{\beta\theta}{8}\left(\dfrac{\beta}{3}+\theta\right)\right\}\\
-C^4\left\{\dfrac{\alpha^5}{32}-\dfrac{\alpha^4\beta}{32}+\dfrac{\alpha^2\gamma}{4}\left(\dfrac{\alpha}{3}-\dfrac{\beta}{4}\right)+\dfrac{\gamma^2}{24}\left(\alpha-\dfrac{\beta}{3}\right)\right\}\\
-C^4\theta\left\{\dfrac{-5\alpha^4}{16}+\dfrac{\alpha^2\beta}{2}\left(\alpha-\dfrac{3\beta}{16}\right)+\dfrac{\gamma}{2}\left(-\alpha(\alpha-\beta)-\dfrac{1}{6}(\beta^2+\gamma)\right)\right\}\\
-\theta^2C^4\left\{\dfrac{5\alpha^3}{4}+9\alpha\beta\left(-\dfrac{\alpha}{4}+\dfrac{\beta}{8}\right)-\dfrac{\beta^3}{8}+\gamma\left(\alpha-\dfrac{3\beta}{4}\right)\right\}\\
-C^4\theta^3\left\{\dfrac{-1}{2}(5\alpha^2+3\beta^2)+4\alpha\beta-\dfrac{2}{3}\gamma+\dfrac{5}{2}\theta(\alpha-\beta)\right\}-C^4\theta^5
\end{array}\right]m^6+O(m^7) \tag{33}$$

The m^1 term is missing in (33), hence *any* TWS + θTS parameter set $\{\alpha, \beta, \gamma, \theta, C\}$ selection yields a discrete solution with first-order phase accuracy for $D \equiv 0$. For order m^2 accuracy, the term coefficient $[1+2\theta+(\alpha-\beta)]$ must vanish. For the time-accurate, non-diffusive Euler TS selection $\theta = 0.5$, the trapezoidal rule, this accrues for any $\alpha = \beta$ for all C. For this θ restriction, order m^3 phase accuracy results for $-\gamma/6 - 1/12 = 0$, hence the optimal value is $\gamma = -0.5$. For these decisions, an order m^4 phase accurate algorithm will result for the term coefficient $\alpha(1-C^2)/24 = 0$, which requires $C = 1$ or $\alpha = 0 = \beta$.

Thereby, the theory predicts the optimally phase-accurate TWS^h + θTS algorithm for the $b = 1$ FE basis implementation accrues to the selections $\alpha = 0 = \beta$, $\theta = 0.5$ and $\gamma = -1/2$. Terming this the TWS-γ algorithm, solutions will be order m^4 phase accurate on a uniform mesh independent of C. Actual TWS^h + θTS algorithm solution accuracy is of course a function of C and mesh non-uniformity.

3.4. Fourier representation in 2D

The TS-modified conservation principle for a 2D pure advection problem ($Pa^{-1} = 0$), recall (12), in a rectangular Cartesian resolution and neglecting the TWS-μ term is

$$\begin{aligned}
\mathscr{L}^m(q) = {} & \frac{\partial q}{\partial t}+u\frac{\partial q}{\partial x}+v\frac{\partial q}{\partial y}-\frac{\alpha\Delta t}{2}\left[\frac{\partial}{\partial x}\left(u\frac{\partial q}{\partial t}\right)+\frac{\partial}{\partial y}\left(v\frac{\partial q}{\partial t}\right)\right]\\
& -\frac{\beta\Delta t}{2}\left[\frac{\partial}{\partial x}\left(u^2\frac{\partial q}{\partial x}\right)+\frac{\partial}{\partial x}\left(uv\frac{\partial q}{\partial y}\right)+\frac{\partial}{\partial y}\left(vu\frac{\partial q}{\partial x}\right)+\frac{\partial}{\partial y}\left(v^2\frac{\partial q}{\partial y}\right)\right]\\
& -\frac{\gamma\Delta t^2}{6}\left[\frac{\partial}{\partial x}\left(u^2\frac{\partial}{\partial x}\frac{\partial q}{\partial t}\right)+\frac{\partial}{\partial x}\left(uv\frac{\partial}{\partial y}\frac{\partial q}{\partial t}\right)+\frac{\partial}{\partial y}\left(vu\frac{\partial}{\partial x}\frac{\partial q}{\partial t}\right)\right.\\
& \left.+\frac{\partial}{\partial y}\left(v^2\frac{\partial}{\partial y}\frac{\partial q}{\partial t}\right)\right]+O(\Delta t^3)=0
\end{aligned} \tag{34}$$

DOI: 10.1002/fld

The amplification factor G^h for the discrete solution $q^h(x, y, t)$ for (33) is again determined *via* assembly of the TWS$^h+\theta$TS algorithm at the generic mesh node (X_j, Y_k). This operation produces a stencil technically similar to (23). The Fourier representations analogous to (25) and (26) are

$$Q_{j-1,k-1} = Q(x-\Delta x, y-\Delta y) = Q_{j,k}\exp(-\mathrm{i}\Delta x\kappa_1)\exp(-\mathrm{i}\Delta y\kappa_2) \tag{35}$$

$$Q_{j+1,k+1} = Q(x+\Delta x, y+\Delta y) = Q_{j,k}\exp(\mathrm{i}\Delta x\kappa_1)\exp(\mathrm{i}\Delta y\kappa_2) \tag{36}$$

for wave number definitions $\kappa_1=\kappa\cos\eta$ and $\kappa_2=\kappa\sin\eta$, recall Figure 1. For the bilinear FE basis implementation of the TWS$^h+\theta$TS algorithm, one thus determines

$$G^h = \frac{(b_{j-1}\mathrm{e}^{-\mathrm{i}\kappa_1}+b_j+b_{j+1}\mathrm{e}^{+\mathrm{i}\kappa_1})\mathrm{e}^{-\mathrm{i}\kappa_2}+(b_{j-1}\mathrm{e}^{-\mathrm{i}\kappa_1}+b_j+b_{j+1}\mathrm{e}^{+\mathrm{i}\kappa_1})+(b_{j-1}\mathrm{e}^{-\mathrm{i}\kappa_1}+b_j+b_{j+1}\mathrm{e}^{+\mathrm{i}\kappa_1})\mathrm{e}^{+\mathrm{i}\kappa_2}}{(a_{j-1}\mathrm{e}^{-\mathrm{i}\kappa_1}+a_j+a_{j+1}\mathrm{e}^{+\mathrm{i}\kappa_1})\mathrm{e}^{-\mathrm{i}\kappa_2}+(a_{j-1}\mathrm{e}^{-\mathrm{i}\kappa_1}+a_j+a_{j+1}\mathrm{e}^{+\mathrm{i}\kappa_1})+(b_{j-1}\mathrm{e}^{-\mathrm{i}\kappa_1}+b_j+b_{j+1}\mathrm{e}^{+\mathrm{i}\kappa_1})\mathrm{e}^{+\mathrm{i}\kappa_2}} \tag{37}$$

The theoretical analysis is tractable only for a uniform mesh, hence $\kappa_1\Delta x\equiv m\equiv\kappa_2\Delta y$, thereby $\Delta x\equiv h\equiv\Delta y$ in (35) and (36) and m remains the non-dimensional wave number. The resultant TS expansion for G^h to order m^4 is detailed in Appendix A.

The exact solution for the 2D pure advection problem is

$$q(x, y, t) = \exp[-\mathrm{i}\{\kappa_1(x-u_x t)+\kappa_2(y-u_y t)\}] \tag{38}$$

for advection velocity vector resolved into Cartesian scalar components. The analytical amplification factor remains the ratio of two successive time interval solutions, hence

$$G_{\text{exact}} = \frac{q(x, y, t_{n+1})}{q(x, y, t_n)} \tag{39}$$

Alternatively, since $\kappa_1=\kappa\cos\eta$ and $\kappa_2=\kappa\sin\eta$

$$G_{\text{exact}} = \exp[-\mathrm{i}m(C_x\cos\eta + C_y\sin\eta)] \tag{40}$$

where C_x and C_y denote the Cartesian resolution of the Courant vector $\mathbf{C}$. The resulting TS expansion to the first three terms in order m is

$$G_{\text{exact}} = 1-\mathrm{i}[C_x\cos(\eta)+C_y\sin(\eta)]m-\tfrac{1}{2}[C_x\cos(\eta)+C_y\sin(\eta)]^2m^2 + \frac{i}{6}[C_x\cos(\eta)+C_y\sin(\eta)]^3m^3+O(m^4) \tag{41}$$

The TWS$^h+\theta$TS algorithm phase remains $c^h=G_{\text{exact}}-G^h$, which is readily approximated from these TS expansions and is detailed in Appendix B to order m^4. As always, stability accrues to bounding $|c^h|=|G|-|G^h|$ by unity. Since $|G|=1$ for the pure advection problem, then $|c^h|=1-|G^h|$ and the resultant solution for phase velocity error to order m^2 is

$$|c^h| = \left(\frac{C_x^2}{2}+C_xC_y+\frac{C_y^2}{2}-\frac{1}{2}(\alpha+\beta)(C_x^2+C_y^2)-\alpha C_xC_y-C_x^2\theta-2C_xC_y\theta-C_y^2\theta\right)m^2 \tag{42}$$

From (42), it is clear that the phase velocity error for *any* TWS$^h+\theta$TS algorithm with definitions $\alpha=0=\beta$ and $\theta=1/2$ will be order m^3 or better. It remains to probe the TS analysis to quantify dependence on phase angle, hence Courant vector $\mathbf{C}$, recall Figure 1.

DOI: 10.1002/fld

4. DISCUSSION AND RESULTS

4.1. *Selected algorithms of the* TWS^h + θTS *class*

With proper interpretations, the TWS^h + θTS construction readily admits recovery of independently derived algorithms, recall Table I, whether they be FE-, FD- or FV-based originally. This class of algorithms generally possesses non-zero, sometimes non-equal values of the TWS parameter set $\{\alpha, \beta\}$, rarely a non-zero γ and may be time explicit or implicit (θ). The comparison algorithms selected include Brooks–Hughes SUPG, explicit TG, GLS, RG, Crank–Nicolson (CN), GWS and the theory-predicted optimal-γ TWS (TWS-γ).

In their original derivations, only the TG($\alpha = 0,\ \beta = 1 = \gamma,\ \theta = 0$) and GLS($\alpha = 2\theta = \beta$, θ arbitrary) algorithms contain Δt and Δt^2 as the term multipliers. TG fits directly, while GLS is recovered by performing a time discretization first, then returning to a continuum form. The algorithms of Dendy, Wahlbin and RG ($\alpha = \beta,\ \gamma = 0$), as established for a hyperbolic model problem, are identical to within Courant number C and mesh measure h. Their conversion to TWS form results by replacing Δt with the local measure of time $h/|u|$, a uniformly non-negative number. The resultant TWS terms in (12), reduced to 1D and for constant u, are

$$\frac{\Delta t}{2}(\alpha u) \equiv \frac{\alpha h u}{2|u|} = \frac{\alpha h \operatorname{sign}(u)}{2}, \qquad \frac{\Delta t}{2}(\beta u u) \equiv \frac{\alpha h u u}{2|u|} = \frac{\alpha h |u|}{2} \tag{43}$$

The local time scale definition implies $C \equiv u\Delta t / h = 1$, which is compensated in the original works by determination of an optimal $\alpha \equiv \beta = v_0$.

The original Brooks–Hughes SUPG algorithm was developed for a steady 1D problem with optimal β. When generalized to the unsteady problem, SUPG is for all intents identical to RG, with the definitions (43) and a constant potentially differing from v_0. The classic FD algorithm CN fits the TWS class for all parameters zero, upon diagonalizing the GWS mass matrix and $\theta \equiv 0.5$.

4.2. TWS^h + θTS *algorithm relative phase error*

The comparison family is thus identified. TG accrues to $\alpha = 0 = \theta$ and $\beta = 1 = \gamma$ in (20). In (32), extremum phase accuracy thus requires $(1 - C^2)/24 = 0$, hence greater than order m^3 accuracy occurs *only* for $C = 1$. In the original RG(SUPG) construction, the reported semi-discrete (only) theoretical analysis [13] determined optimal phase accuracy accrues to $\alpha = 2/(C\sqrt{15}) = \beta$. That $\beta > 0$ results guarantees infusion of an artificial dissipation mechanism, which will be proven. The class of GLS constructions results for $\alpha = 2\theta = \beta$ which fixes the order m^3 coefficient at $-1/12$, thereby yielding at best order m^2 phase accuracy. The final algorithms considered are GWS and TWS-γ for which the theory predicts order m^3 and m^4 phase accuracy, respectively.

For these six TWS^h + θTS algorithms, the solution for phase velocity error, i.e. the difference between unity and (28), as well as the departure of amplification modulus from unity, are graphed in Figure 2(a) for $C = 0.5$. The abscissa semi-log scale, demarked on integer multiples of h, improves resolution distinction in the all-important short-wavelength region. Except for TG, which exhibits zero phase velocity dependence on wavelength λ, all other TWS^h + θTS algorithms possess lagging phase error for all λ and, as anticipated, 100% error at $\lambda = 2h$. In the interval $2h < \lambda \leqslant 3h$, GLS and RG(SUPG) exhibit minimal phase velocity error, but thereafter lose superiority to TWS-γ. CN exhibits the largest phase error throughout, and the TWS-γ phase error is minimal for all $\lambda > 4h$ (except for TG).

DOI: 10.1002/fld

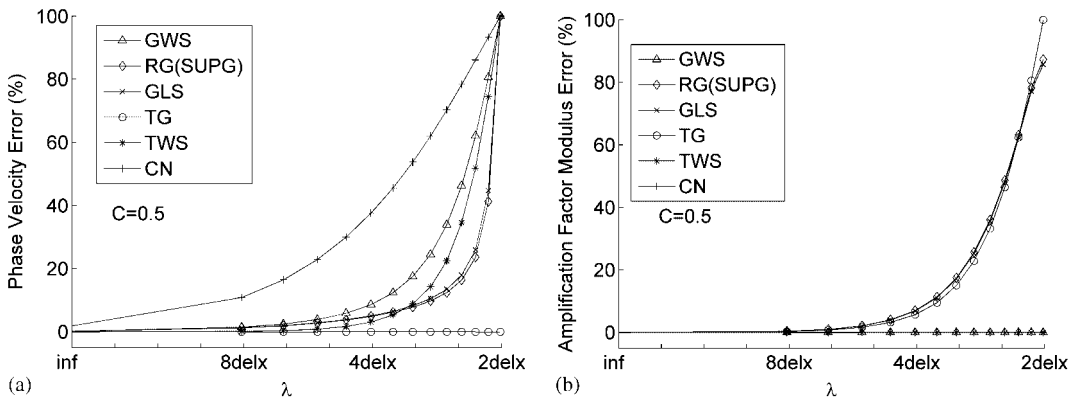

Figure 2. Phase velocity and amplification factor modulus error, 1D pure advection, $C = 0.5$, $\theta = 0.5$ (except for TG).

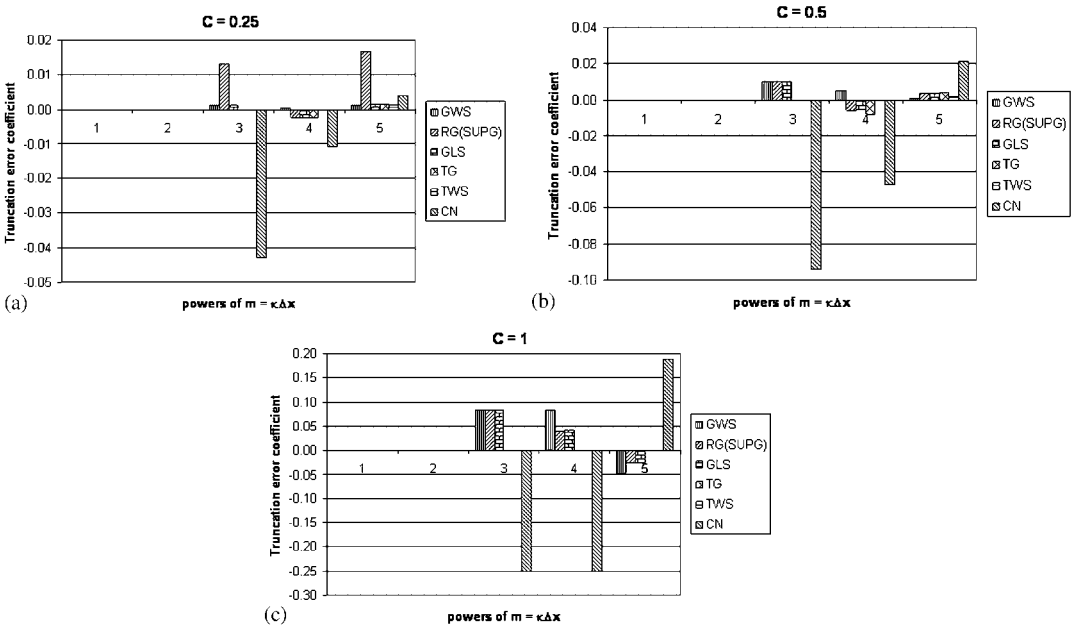

Figure 3. TWS algorithm discrete solution TS coefficients in non-dimensional wave-number space, 1D pure advection: (a) $C = 0.25$; (b) $C = 0.5$; and (c) $C = 1.0$.

The bar chart presentations in Figure 3(a)–(c) compare the magnitude of the theory TS coefficient, for each wave number order m^{α}, for Courant numbers $C = 0.25$, 0.5 and 1.0. For $C = 0.25$ and 0.5, the progression in decreasing phase inaccuracy is TWS-γ, TG, GWS, GLS, RG(SUPG) and CN. At $C = 1.0$, the order is TWS-γ, TG, RG(SUPG), GLS, GWS and CN. Clearly then, the theory

DOI: 10.1002/fld

predicts that the TWS-γ algorithm is the optimal linear basis FE implementation of all selected TWS + θTS formulations.

The remaining issue of theoretical importance is algorithm stability, which requires $|G^h| \leqslant 1$. The exact solution possesses $|G| = 1$, and the spectral distribution of the TWS^h + θTS algorithm error modulus is $|e^h| = |G^h| - |G|$. Figure 2(b) graphs these solutions for $|e^h|$ for the six algorithms. GWS, TWS-γ and CN exhibit zero error for all wavelengths, hence possess no numerical diffusion. At $\lambda = 2h$, the modulus error for TG is 100% and for GLS and RG(SUPG) is 87%. Thereby, the superior short-wavelength phase error accuracy of these two algorithms comes at the expense of a very large level of numerical diffusion.

4.3. Unsteady pure advection in 1D

Numerical comparisons of algorithm performance accrues to propagation of a smooth or non-smooth initial condition (IC) by a constant imposed velocity u. The analytical solution (28), simplified for vanishing diffusion coefficient D in 1D, is

$$q(x, t) = \exp[\mathrm{i}\kappa(x - ut)] \tag{44}$$

which confirms that *any* IC $q(x, t_0)$ will propagate *absolutely unaltered* parallel to the x axis with speed u. Thereby, this problem statement belongs to the verification class, as the exact solution is known for all C.

For IC the (smooth) gaussian, and propagated over three IC wavelengths downstream of the IC position, TWS^h + θTS algorithm solutions are compared to the exact solution in Figure 4(a)–(e) for $C = 0.5 = \theta$, except TG which retains the definition $\theta = 0$. Clearly, the most accurate solution in the *eyeball norm* is TWS-γ, followed in order by TG, GWS, RG(SUPG), GLS and CN. The theory predicts that the RG(SUPG) and GLS($\theta = 0.5$) phase velocity and amplitude error distributions are very similar, Figure 2, which is visually confirmed by the data in Figure 4.

The developed theory precisely predicts this relative performance. Table II lists the computed nodal extrema for each algorithm tested for $C = 0.5$ and 1.0. Except for TWS-γ and TG, algorithm performance degrades for larger C, with additional loss of peak value and larger dispersion error-induced lagging phase error.

The theory further predicts that solution quality improves/degrades for use of smaller/larger Courant numbers. Figure 5(a)–(e) summarizes solutions for gaussian IC propagation compared to the exact solution for $C = 1$. Except for TWS-γ and TG, solution fidelity degenerates significantly in the *eyeball norm*, with CN the worst performer. The theory prediction that both TWS-γ and TG solutions are essentially nodally exact is clearly evident at $C = 1$. Further, for the IC a non-smooth square wave, both algorithms still generate nodally exact solutions on a uniform mesh at $C = 1$, Figure 6, which will occur for *any* IC.

4.4. Theory improvements to published algorithms

The TWS^h + θTS theory provides the opportunity to optimize phase accuracy for algorithms in the class. For example, the order m^4 truncation error coefficient $C^2(\alpha - 2C^2)/24$ can be minimized while retaining $\alpha = \beta$ for RG(SUPG) and GLS. The formulations remain Courant number dependent, specifically for $C = 1$ optimal $\alpha = 2 = \beta$, while for $C = 0.5$ the value is 0.5, and the modified algorithms thereby match the optimal phase accuracy order associated with TWS-γ.

Another example is the classical CN algorithm [25]. The distinguishing characteristic of the FE linear basis implementation of TWS^h + θTS, compared to CN, is the non-diagonal mass matrix

DOI: 10.1002/fld

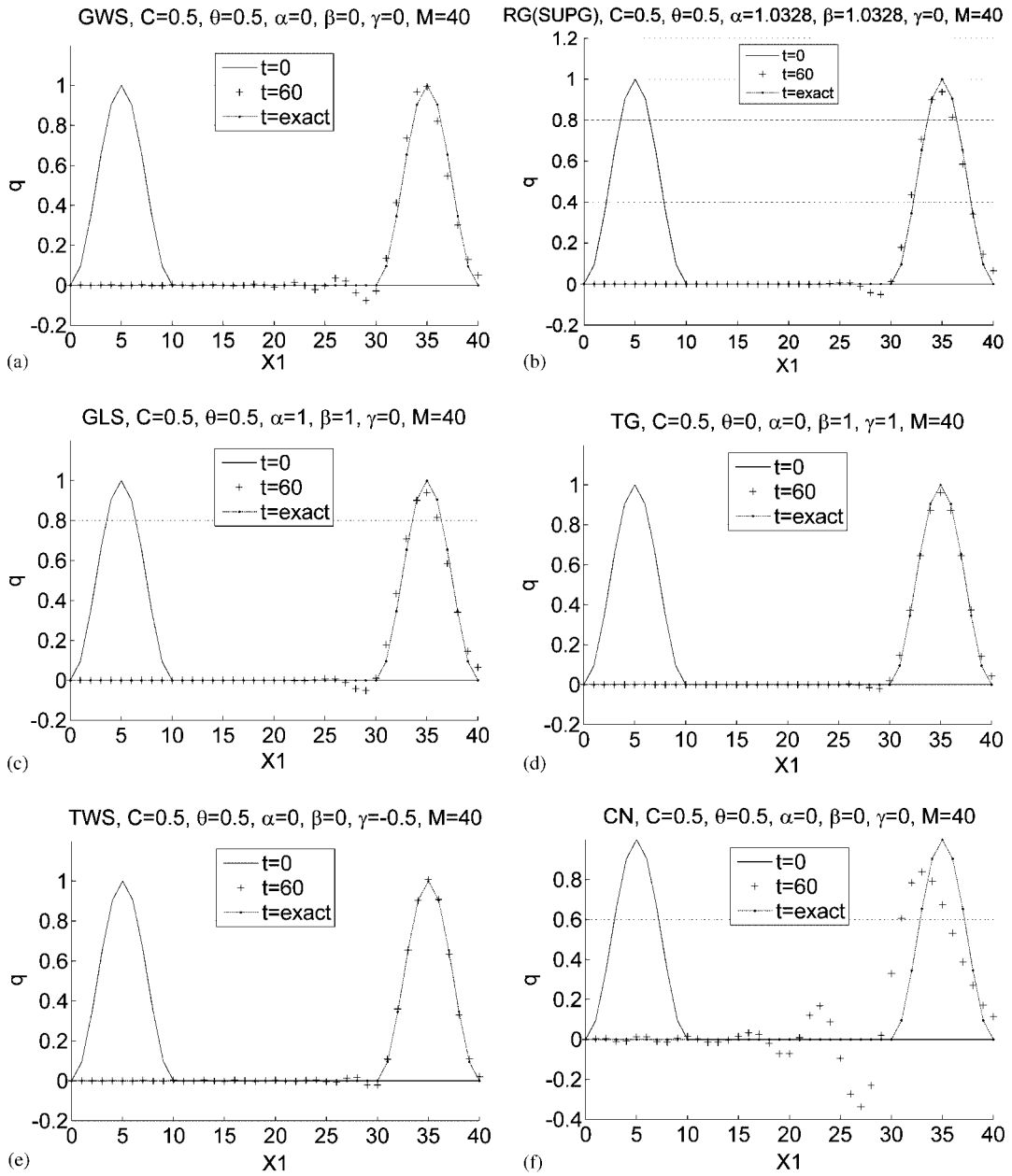

Figure 4. 1D pure advection of a Gaussian IC, $C = 0.5$, dashed line is exact solution, following 3-IC-wavelength translation.

DOI: 10.1002/fld

Table II. Solution nodal extrema after 3-wavelength translation, Gaussian IC, 1D pure advection.

		Max	Min
$C=0.5$	GWS	0.9938	−0.0767
	RG(SUPG)	0.9385	−0.0508
	GLS	0.9398	−0.0516
	TG	0.9608	−0.0207
	TWS-γ	1.0087	−0.0210
	CN	0.8397	−0.3374
	CNm	0.8556	−0.3207
$C=1.0$	GWS	0.9496	−0.1765
	RG(SUPG)	0.9194	−0.1458
	GLS	0.8988	−0.1171
	TG	1.0	0.0
	TWS-γ	1.0	0.0
	CN	0.7989	−0.3649
	CNm	0.8640	−0.3104

in (15). Diagonalizing the mass matrix, a commonly examined form in the FE literature, and then proceeding through the theory process yields

$$G^h_{\mathrm{CNm-FD}} = 1 + \frac{3\beta C^2(\cos m + 1) - \mathrm{i}3C\sin m}{(3+\gamma C^2 + 3\theta\beta C^2) - C^2(\gamma + 3\theta\beta)\cos m + \mathrm{i}3C\left(\dfrac{-\alpha}{2}+\theta\right)\sin m} \tag{45}$$

The corresponding CN-modified (CNm) algorithm phase error TS through third order is

$$\begin{aligned} c^h_{\mathrm{CNm-FD}} = {} & -2(C^2\beta) - \mathrm{i}C[1+(1+C^2\alpha\beta-2C^2\beta\theta)]m \\ & + C^2\left[-\frac{1}{2}-\frac{1}{2}(\alpha-\beta)-\frac{1}{3}C^2\beta\gamma+\theta(1-C^2\beta^2)-2\beta C^2\left(-\frac{\alpha^2}{4}-\frac{\gamma}{3}+\theta(\alpha-\beta-\theta)\right)\right]m^2 \\ & + \mathrm{i}\left[\frac{C^3}{6}-\left(\frac{C}{6}+C^3\left(-\frac{5}{12}\alpha\beta-\frac{\gamma}{6}+\frac{1}{3}\beta\theta\right)\right)\right. \\ & \left. - C^2(-C+C^3\beta(\alpha-2\theta))\left(-\frac{\alpha^2}{4}-\frac{\gamma}{3}+\theta(\alpha-\beta-\theta)\right)\right]m^3+\mathrm{O}(m^4) \end{aligned} \tag{46}$$

From (46), first-order phase accuracy requires $\beta=0$, whereupon the order m^2 TS coefficient becomes $C^2(-1/2+\theta)$, which is annihilated by setting $\theta=0.5$, as in the original CN formulation. The order m^3 coefficient becomes $C^3(-1/12-\gamma/3)-C(1-C\gamma)/6$, which will not vanish for any γ or C. As occurred with the theory-modified RG(SUPG) and GLS algorithms, an optimal γ can be chosen dependent on C. Specifically, for $C=1$ the optimal γ is -0.5, while for $C=0.5$ order m^3 phase accuracy is independent of γ. Note, however, that this CNm algorithm cannot match the m^4 order of the optimal TWS-γ algorithm.

DOI: 10.1002/fld

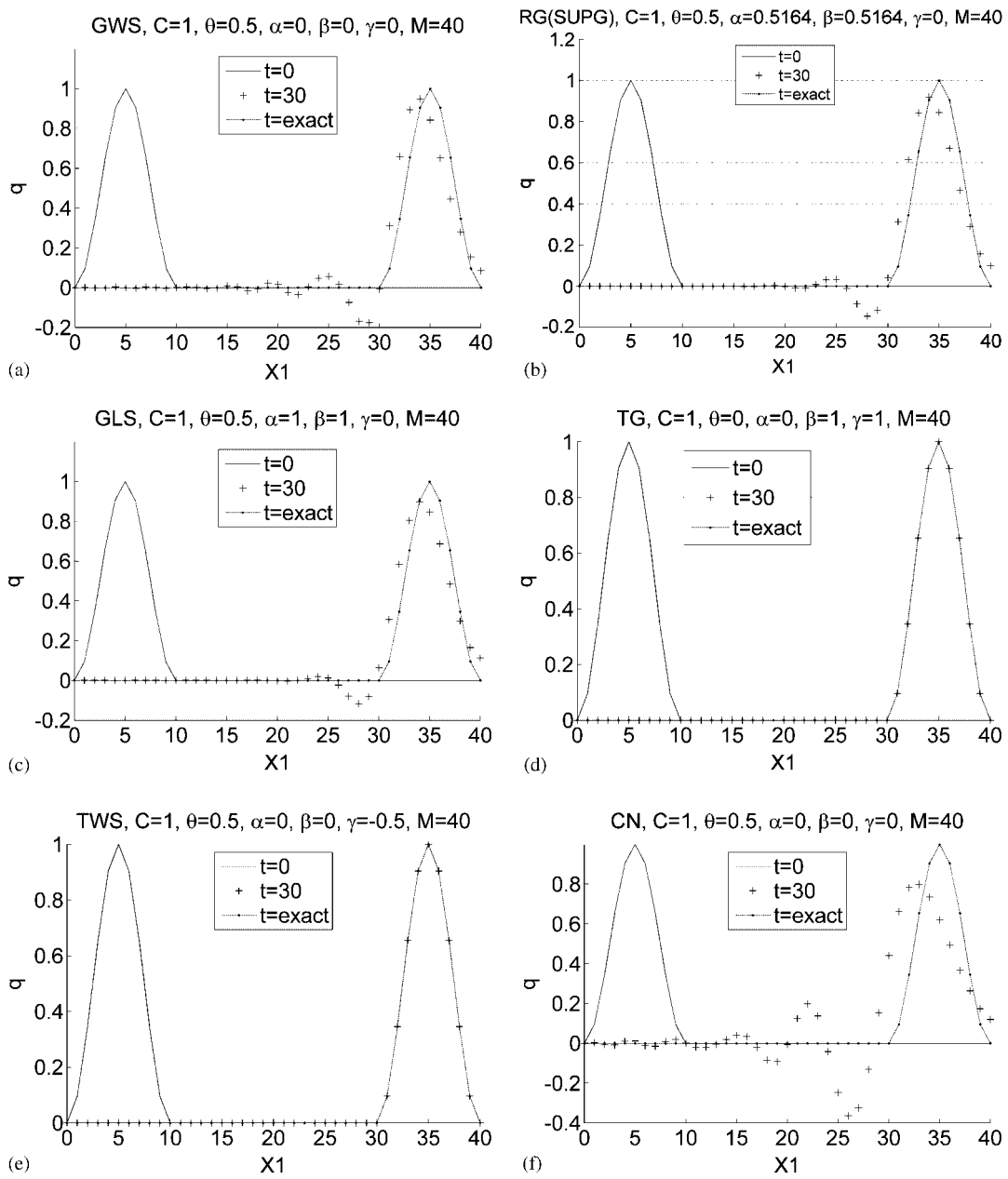

Figure 5. 1D pure advection of a Gaussian initial distribution, $C = 1.0$, dashed line is exact solution following 3-wavelength translation.

DOI: 10.1002/fld

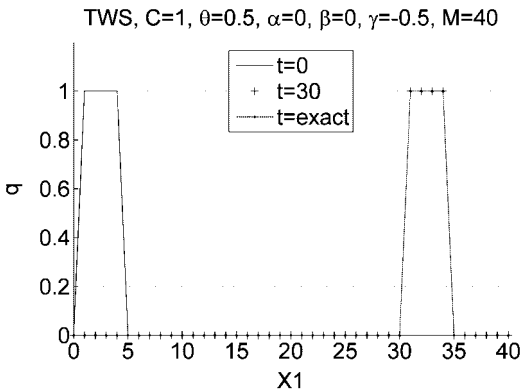

Figure 6. 1D pure advection of a square wave IC for TWS-γ, $C = 1.0$, dashed line is exact solution following 7-wavelength translation.

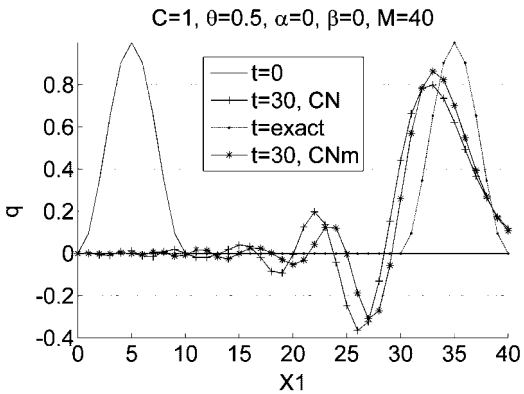

Figure 7. 1D pure advection of a Gaussian initial distribution for CN and CNm, $C = 1.0$, dashed line is exact solution following 3-wavelength translation.

For the gaussian IC verification problem, solutions generated *via* the TWS theory-optimized CNm algorithm are improvements over those generated by classical CN, Figure 7, see also Table II. Although the improvement is truly modest, that it was predicted by the developed theory is the key result.

4.5. Identified TWS$^h + \theta$TS *algorithm theory anomalies*

During evaluation of the presented theory, anomalies for certain algorithms departing from expected performance have been observed. Recalling (23) as the general statement of the TWS$^h+\theta$TS stencil, linear FE basis implementations of both the TWS-γ and TG algorithms, when assembled at the generic node X_j for $C = 1$, produce (23) in the form

$$(Q_j + Q_{j+1})_{n+1} = (Q_j + Q_{j-1})_n \tag{47}$$

DOI: 10.1002/fld

Recalling that n is the time-step index, (47) states precise transport of nodal data over one mesh interval at each time step on a uniform mesh at $C=1$ and any IC. Thereby, the recorded $C=1$ algorithm performance for any IC is not a surprise.

Repeating this process for the derived RGm (SUPGm) algorithm, while retaining arbitrary $\alpha \equiv \beta$, assuming γ small and setting $\theta = 0.5$ yields (23) in the form

$$-\frac{1}{12}Q_{j-1}^{n+1} + \left(\frac{\alpha}{2} + \frac{2}{3}\right)Q_j^{n+1} + \left(-\frac{\alpha}{2} + \frac{5}{12}\right)Q_{j+1}^{n+1}$$
$$= \left(\frac{\alpha}{2} + \frac{5}{12}\right)Q_{j-1}^{n} + \left(-\frac{\alpha}{2} + \frac{2}{3}\right)Q_j^{n} - \frac{1}{12}Q_{j+1}^{n} \tag{48}$$

For sufficiently large α, (48) takes the approximate form

$$-\frac{1}{12}Q_{j-1}^{n+1} + \left(\frac{\alpha}{2}\right)Q_j^{n+1} + \left(-\frac{\alpha}{2}\right)Q_{j+1}^{n+1} \approx \left(\frac{\alpha}{2}\right)Q_{j-1}^{n} + \left(-\frac{\alpha}{2}\right)Q_j^{n} - \frac{1}{12}Q_{j+1}^{n}$$

which, upon obvious term cancellation, predicts exact propagation of nodal data at $C=1$. Figure 8 confirms the theory prediction for propagation of the gaussian IC for $\alpha = 100 = \beta$, as the RGm (SUPGm) and exact solutions are very close. However, such large values of $\{\alpha, \beta\}$ eliminate the base algorithm terms, hence are not at all practical.

Among the considered TWS^h + θTS algorithm class, TWS-γ, TG and RGm (SUPGm) each exactly propagate nodal data at $C=1$. This occurrence requires a solution of the amplification factor phase velocity and modulus spectral distribution. Viewing Figure 9(a), the theory predicts a discontinuous jump in phase velocity error, switching from substantial leading on $2h<\lambda\leqslant 4h$ to near zero lagging for all wavelengths $\lambda>4h$. The RG(SUPG) and GLS algorithms also exhibit this phenomenon, however, the associated solutions are not nodally exact due to the associated large artificial diffusion present, Figure 9(b). The GWS and CN algorithms exhibit lagging phase error at all wavelengths, which totally prevents exact propagation of nodal data.

Any TWS^h + θTS algorithm implemented with $\theta>0.5$ inherits a numerical diffusion mechanism, since $|G^h|<1$ for this selection. The bounding case is $\theta = 1$, for which the phase velocity and

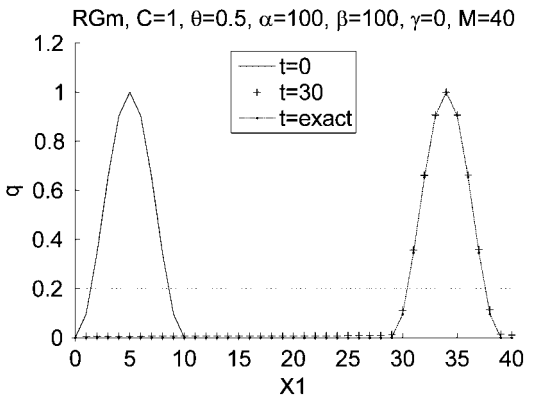

Figure 8. 1D pure advection of a Gaussian initial distribution, $C=1.0$, RGm with $\alpha = 100 = \beta$, dashed line is exact solution following 3-wavelength translation.

DOI: 10.1002/fld

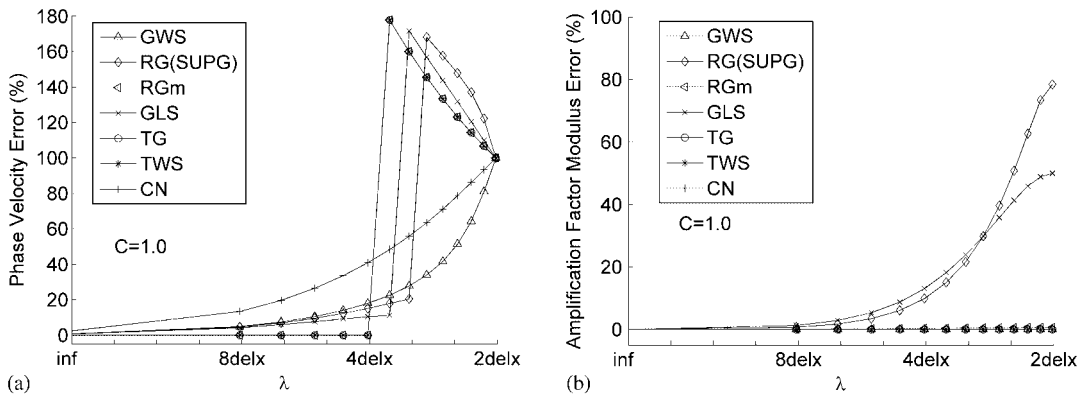

Figure 9. Phase velocity and amplification factor modulus error, $C = 1.0$ and $\theta = 0.5$.

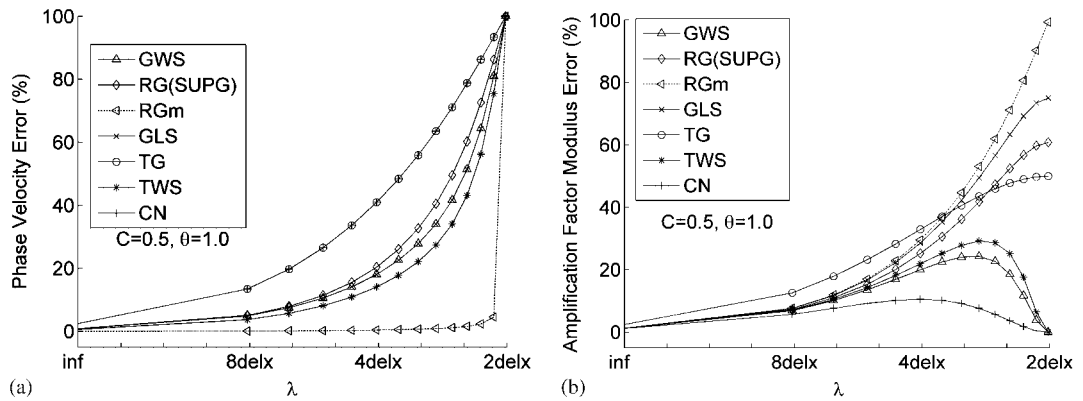

Figure 10. Phase velocity and amplification factor modulus error, $C = 0.5$ and $\theta = 1.0$.

modulus error distributions for $C = 1$ are graphed in Figure 10(a) and (b). The RGm (SUPGm) algorithm now exhibits zero phase error for all $\lambda > 2h + \varepsilon$, but the extremum distribution of modulus error coexists. All other algorithms retain the expected wavelength-dependent distributions for phase velocity. The other interesting prediction is zero modulus error for the GWS, TWS-γ and CN algorithms at $\lambda = 2h$, with the CN algorithm exhibiting minimal error over the wavelength spectrum. One can conclude that these algorithms will not perform acceptably, as verified by the verification problem solutions discussed.

An additional occurrence of anomalous theory prediction, detailed in Sahu [26], resulted from use of a canned optimization code [27]. Clearly, prediction of optimal TWS theory parameter sets depends totally on code robustness. The interesting result from this exercise was the prediction of $\theta < 0.5$, classically unstable, upon inputting large TWS coefficients $\{\alpha, \beta\}$ at search initiation. Specifically, for initiation at $\alpha = 100 = \beta$, $\gamma = 0$ and $\theta = 0.5$, the code returned $\alpha = 100.048$, $\beta = 100.0532$, $\gamma = 0.27067$ and $\theta = 0.49743$. Substituting this prediction into (29), the fractional

DOI: 10.1002/fld

Table III. Solution nodal extrema after 25 time steps, Gaussian IC, 1D advection–diffusion, $Pe = 10,\ 1000;\ C = 1,\ M = 40$.

	$C = 1$			
	$Pe = 10$		$Pe = 1000$	
	Max	Min	Max	Min
Exact	0.684000	0	0.995090	0
GWS	0.679990	−1.422E−02	0.966789	−1.4810E−01
RG(SUPG)	0.674538	−5.207E−03	0.931993	−1.1942E−01
GLS	0.681359	−9.816E−04	0.908791	−9.8639E−02
TG	4.362461	−4.523E+00	0.996144	−5.8300E−06
TWS-γ	0.689254	−6.042E−05	0.995248	−5.4484E−10
CN	0.645886	−1.058E−01	0.833308	−3.4159E−01

$\{\alpha, \beta\}$ difference is compensated by $\theta < 0.5$, which minimizes the order m^2 TS coefficient, while $\gamma = 0.27067$ minimizes the order m^3 TS coefficient.

4.6. Unsteady advection–diffusion in 1D

Now including physical diffusion, for a smooth gaussian IC distribution, the verification problem analytical solution is [21]

$$q(x, t) = \frac{\exp[-(x - x_0 - t)^2/2(1 + 2t/Pe)]}{\sqrt{(1 + 2t/Pe)}} \tag{49}$$

where Pe is the Peclet number. Sahu [26] has shown that for $Pe = 10$ and $\theta = 0.5$, after 25 time steps at $C = 1$, both the GWS and RG(SUPG) solutions exhibit a small dispersive lagging phase error. The GLS solution is devoid of dispersion error, the algorithm distinction being the larger $\alpha = \beta$, recall Table I. The TG $\theta = 0$ solution is unstable, while the CN solution exhibits a large dispersion error with lagging phase. The TWS-γ and GLS solutions slightly over/under predict the analytical peak and both are visually monotone. For this problem specification, the accuracy performance order in solution extrema is TWS-γ/GLS, RG(SUPG), GWS, CN, TG, Table III.

For $Pe = 1000$, the problem is advection dominated, hence maintaining accuracy is more challenging. Based on the theory, one expects the TWS-γ algorithm will yield optimum solution fidelity. This is indeed true; for $Pe = 1000$, the accuracy performance order in solution extrema is TWS-γ, TG, GWS, RG(SUPG), GLS, CN, Table III. It is no surprise that this order is identically that observed for the pure advection case.

Finally, decreasing the time step size to $C = 0.5$ indeed improves accuracy across all algorithms. Of note, recalling that TG was unstable for $C = 1.0$ and $Pe = 10$, it now performs second to TWS-γ. These results highlight the limitation of the TG algorithm being time explicit.

4.7. Theory for pure advection in 2D

In proceeding to multi-dimensions, the basic requirement is to probe the TWS^h + θTS theory TS wave number expansion, (37), to quantify phase angle and Courant vector $\mathbf{C}$ dependencies, recall Figure 1. Figure 11 presents the sample space of wave vector angles $\eta = \pi/2, 5\pi/8, 3\pi/4, \pi, 5\pi/4$

DOI: 10.1002/fld

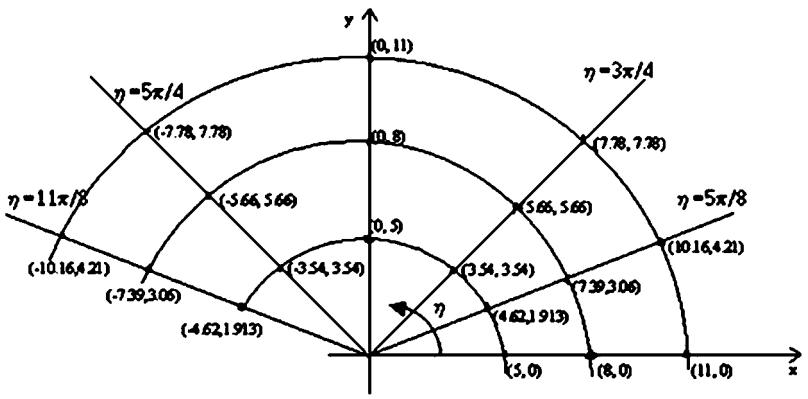

Figure 11. Sample space of wave vector angles for TS theoretical error quantization.

and $11\pi/8$, along with sample geometric coordinates for $0.19 \leqslant |\mathbf{C}| \leqslant 0.41$. The theory predicts algorithm error is angular quadrant independent, even though $\mathbf{C} = (r\omega\Delta t/h)\hat{\mathbf{e}}$ is indeed a vector, where ω is angular velocity and $\hat{\mathbf{e}}$ is the unit vector tangent to the η direction. This prediction is in agreement with the results in Christon *et al.* [7, 8].

A manipulation of the $\{\alpha, \beta\}$ coefficient set terms in (12) are required to recover the resolved form of SUPG reported in Brooks–Hughes [15], hence also RG if its development had been multi-dimensional. Since velocity is a vector, and a multi-dimensional FE possesses at least two mesh measures, the local time scale generalization for TWS would be $\Delta t \equiv |u_i|h_i/u^2 = |\widehat{u}_i|h_i/|\mathbf{u}|$, a non-negative number, with summation on the repeated index and h_i the mesh scale in the direction of u_i. The modifications to the pertinent TWS terms in (12), companion to (43), would be

$$\frac{\Delta t}{2}(\alpha u_j) \equiv \frac{\alpha h_i |u_i| u_j}{2u^2} = \frac{\alpha h_i |\widehat{u}_i| \widehat{u}_j}{2}, \quad \frac{\Delta t}{2}(\beta u_j u_k) \equiv \frac{\alpha h_i |u_i| u_j u_k}{2u^2} = \frac{\alpha h_i |\widehat{u}_i| \widehat{u}_j u_k}{2} \tag{50}$$

where superscript 'hat' signifies the associated unit vector.

For the range of TWS^h + θTS algorithms considered to here, Figure 12(a)–(c) comparatively graphs each algorithm TS coefficient magnitude, for direction $\eta = 3\pi/4$ and $0.19 \leqslant |\mathbf{C}| \leqslant 0.41$, over the order range of non-dimensional wave number m. Figure 13(a)–(c) presents the companion data for $\eta = 5\pi/8$. The dominant error order for RG(SUPG), GLS and TG is m^2 for *all* η and $|\mathbf{C}|$ and the associated TS coefficients are each relatively large. In distinction, the lead error order for GWS, CN and TWS-γ is m^3. Since the TS coefficient magnitudes for CN are exceptionally large, Figures 12(d) and 13(d) graph only the GWS and TWS-γ data for an improved comparison.

One key observation is that the order m^4 error associated with TWS-γ in 1D is degraded to order m^3 in 2D (and 3D). However, as algorithm solution fidelity is dominated by the non-vanishing TS coefficient lowest order in m, the theory still predicts TWS-γ is optimal, as this coefficient is from 1/2 to 1/5 that of GWS. The same comment holds for the m^4 coefficients, while the m^5 coefficient being small and nominally identical is of marginal practical impact. As the final caveat, both the TWS-γ and TG algorithm TS order m^3 coefficients vanish for η aligned with a coordinate axis, i.e. the 1D form already established.

In summary, TWS-γ exhibits the minimum magnitude TS coefficient for all orders m, η, $|\mathbf{C}|$ and coordinates tested. Thereby, the theory again predicts that TWS-γ algorithm solutions will be

DOI: 10.1002/fld

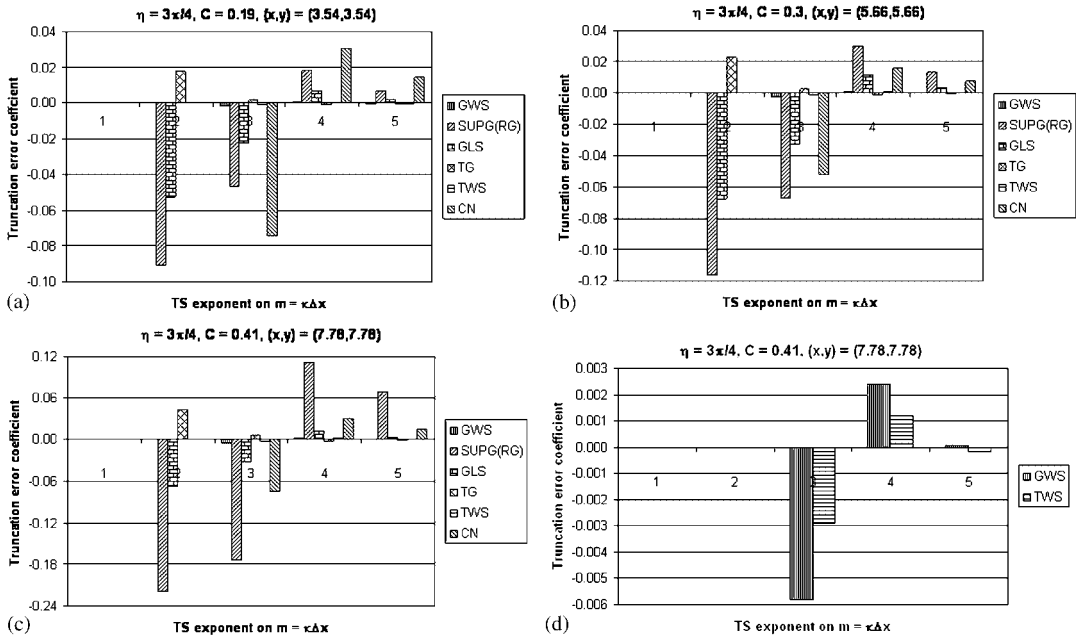

Figure 12. Theoretical Taylor series wave number dependence for TWS$^h + \theta$ TS algorithms, 2D pure advection, $\eta = 3\pi/4$, $0.19 < C < 0.41$.

optimally accurate among the class considered. Hence, there exists little incentive to further consider RG(SUPG), GLS or CN. As a final comparison, Figure 14 quantifies order m distinctions for GWS *versus* TWS-γ on $\pi/2 \leqslant \eta \leqslant 3\pi/4$ and extremum $|\mathbf{C}| = 0.41$. Note the zero TS coefficients for orders m^3 and m^4 for TWS-γ on $\eta = \pi/2$, again due to coordinate alignment. Predicted solution fidelity is clearly dependent on $|\mathbf{C}|$. Comparing the data in Figures 11–13, the lead order TS coefficient magnitudes are roughly three times larger at $|\mathbf{C}| = 0.41$ than at $|\mathbf{C}| = 0.19$, which provides an estimate of Courant number effect on error.

4.8. A pure advection verification in 2D

The definitive verification problem is the rotating cone [28] defining pure advection of a mass distribution $q(\mathbf{x}, t)$ on a 2D solution domain Ω. On domain boundary segments $\partial\Omega$ experiencing inflow, the BC is $q(\mathbf{x}_b, t) = q_b = 0$. Conversely, on segments with outflow the BC is homogeneous Neumann, i.e. $\hat{\mathbf{n}} \cdot \nabla q = 0$. The IC is $q(\mathbf{x}, t_0) = 0$ on $\Omega \cup \partial\Omega$ except for an isolated non-zero IC distribution which is circularly advected around Ω by imposition of the solid body rotation velocity vector field $\mathbf{u}(x, y) = \mathbf{u}(r) = r\omega\hat{\mathbf{e}}_{\boldsymbol{\theta}}$. Here, r is the radial coordinate with origin at the centre of Ω, ω is the angular frequency and $\hat{\mathbf{e}}_{\boldsymbol{\theta}}$ is the unit vector tangent to the angular direction, recall Figure 11. The resultant Courant vector $\mathbf{C} = C\hat{\mathbf{e}}_{\boldsymbol{\theta}} = \sqrt{(C_x^2 + C_y^2)}\hat{\mathbf{e}}_{\boldsymbol{\theta}}$ is distributed as a linear function of radius r.

The smooth IC for the rotating cone problem is a gaussian, illustrated in perspective in Figure 15. This distribution is also identical to the exact solution following any motion induced by the imposed

DOI: 10.1002/fld

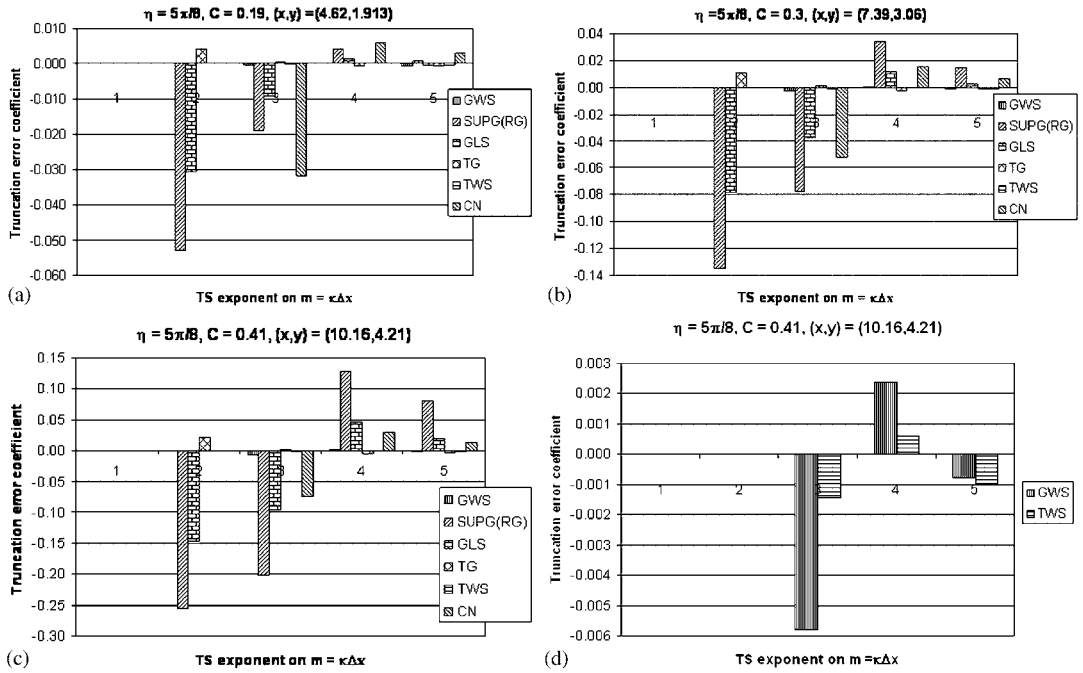

Figure 13. Theoretical Taylor series wave number dependence for $\mathrm{TWS}^h + \theta$ TS algorithms, 2D pure advection, $\eta = 5\pi/8$, $0.19 < C < 0.41$.

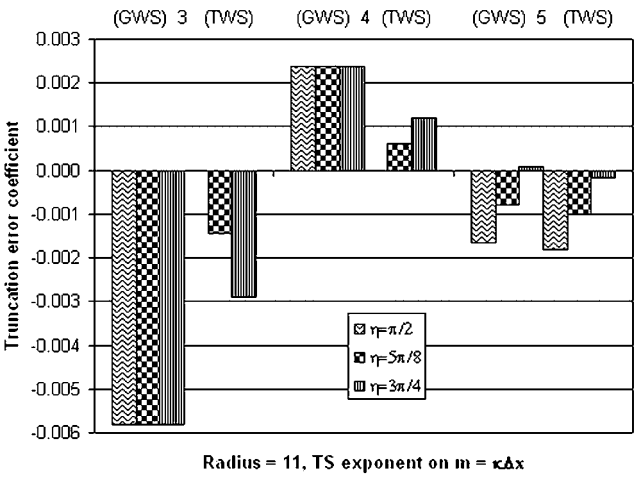

Figure 14. Theoretical Taylor series wave number dependence for GWS^h, $\mathrm{TWS}^h + \theta$ TS algorithms, 2D pure advection, $\eta = \pi/2$, $5\pi/8$, $3\pi/4$, $|\mathbf{C}| = 0.41$.

DOI: 10.1002/fld

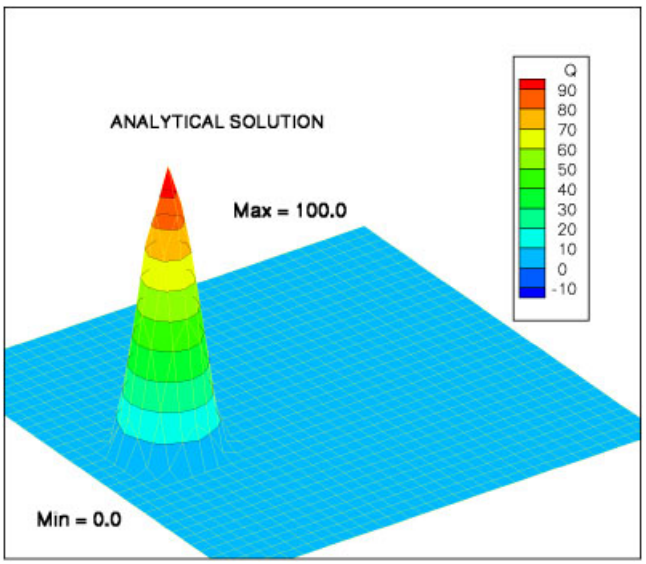

Figure 15. Gaussian IC and exact solution for the rotating cone verification problem.

velocity vector field. The computational experiments are conducted for exactly the time interval required for the analytical solution to complete one circulation around Ω, whence the exact solution remains precisely identical to the IC, Figure 15. The Courant vector magnitude at the cone centroid is $|\mathbf{C}| = 0.3$, and the range over the IC distribution is $0.19 \leqslant |\mathbf{C}| \leqslant 0.41$.

For the FE bilinear basis implementation of each considered TWS$^h + \theta$TS algorithm, Figure 16 graphs in perspective the resultant solutions after the precise time for the analytical solution to make one circuit around the domain Ω. The mesh for each solution is uniform rectangular cartesian. The TWS algorithm particulars for each method are listed in the figure header and the extremum solution values are appropriately recorded. In the *eyeball norm*, TWS-γ produces the most accurate solution in all comparison bases, i.e. reaching the correct location, preservation of the sharp peak value (100), distribution symmetry and minimal magnitude (-6.5) dispersion error-induced wake. In the order of decreasing solution accuracy with (peak, wake) magnitude are GWS(94, -15.3), SUPG(RG)(89.2, -11.6), TG(83.3, -3.4), GLS(81.9, -4.6) and lastly CNFD(44.6, -27.9). Since the TWS $\{\alpha, \beta\}$ term operators are {dispersive, diffusive}, the action of diffusive moderation of dispersion error is clearly illustrated. For corroboration, Brookes–Hughes [15] report their SUPG solution peak to be 88. Finally, the non-diffusive CNFD algorithm suffers rampant dispersion error distortion, as theoretically predicted by the large TS coefficient on the order m^2 term.

These data confirm that TWS-γ produces the optimally accurate solution for the rotating cone, in comparison to the considered algorithms. To evaluate the impact of an unstructured mesh implementation, the TWS algorithm was reformed using the FE natural coordinate (triangle) linear basis, and simulations executed on the same bilinear basis mesh with each uniform quadrilateral bisected into two triangles. Figure 17 graphs in perspective the resultant solutions generated for TWS-γ, GWS and TG. Each algorithm solution suffers a modest degradation in accuracy, quantified in Table IV in terms of extremum nodal values. For either FE basis implementation, the theoretical prediction that the TWS-γ solution is optimal in the class is fully verified.

DOI: 10.1002/fld

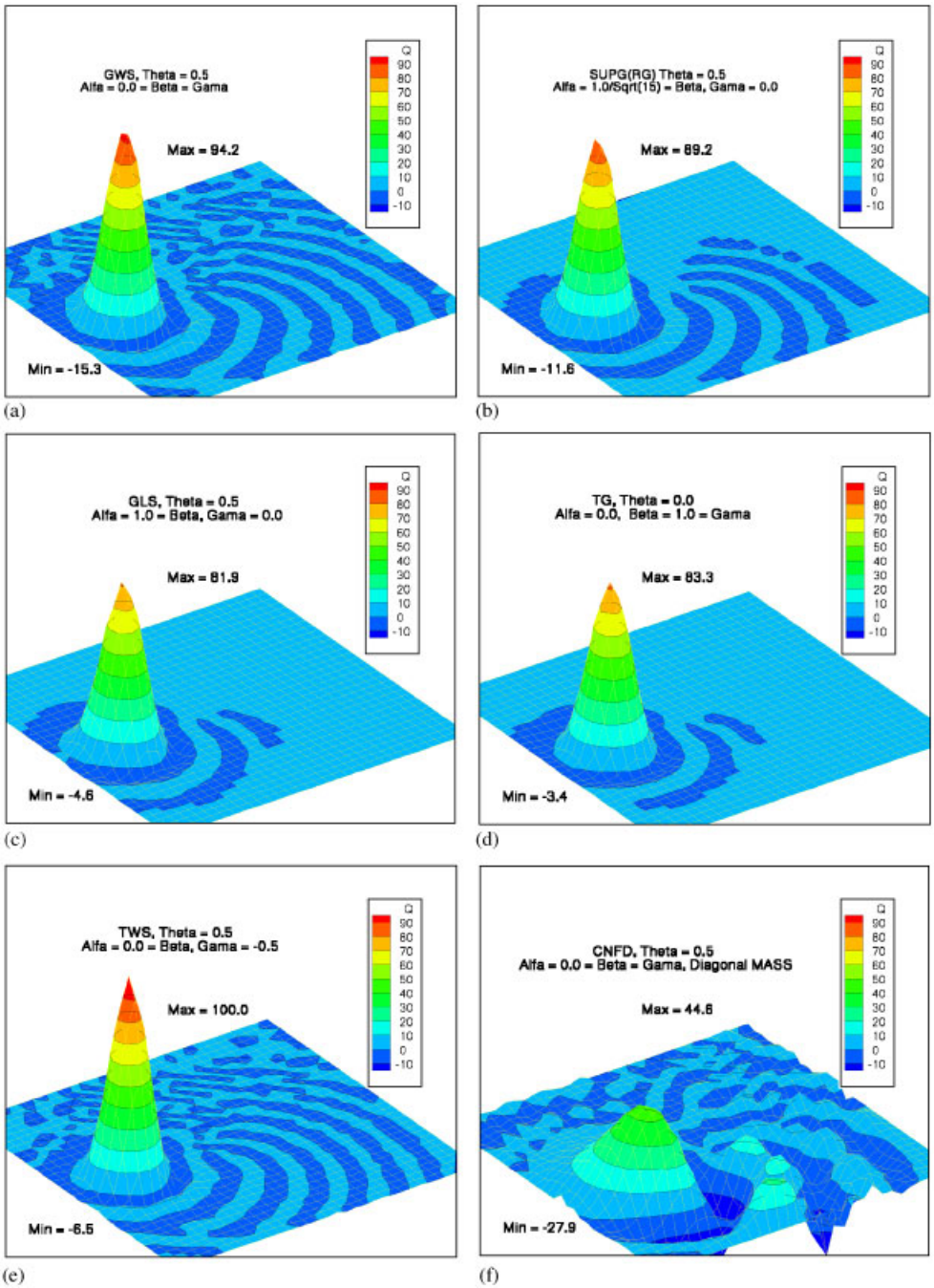

Figure 16. 2D pure advection rotating cone verification problem, discrete solutions after one revolution, uniform Cartesian mesh, $|\mathbf{C}| = 0.3$ at IC centroid.

DOI: 10.1002/fld

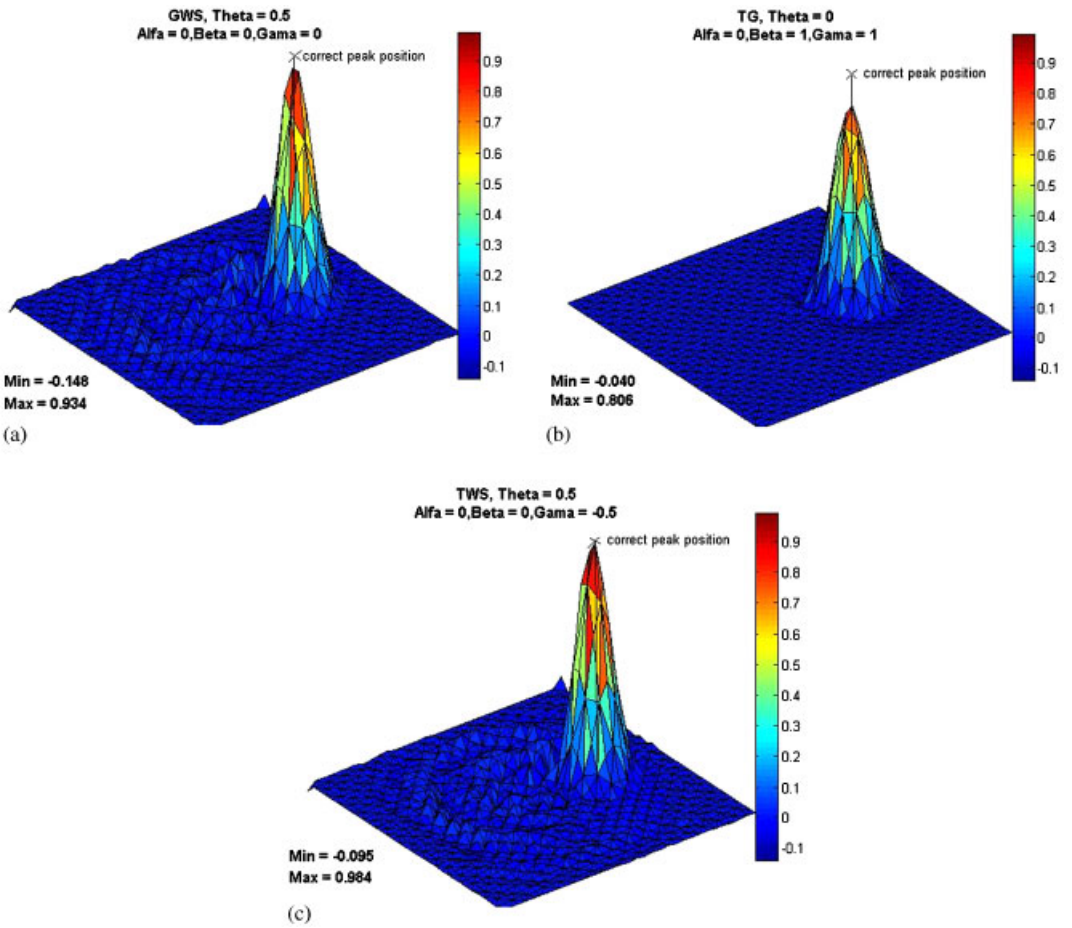

Figure 17. 2D pure advection rotating cone verification problem, discrete solutions after one revolution, uniform triangular mesh, $|\mathbf{C}| = 0.3$ at IC centroid.

Table IV. 2D pure advection, algorithm nodal extrema after one rotation, $|\mathbf{C}| = 0.3$ at IC centroid, FE bilinear and natural coordinate linear basis implementations.

						Uniform Cartesian mesh		Uniform triangular mesh	
	α	β	γ	θ	$\lvert\mathbf{C}\rvert$	Max	Min	Max	Min
TWS-γ	0	0	-0.5	0.5	0.3	100.0	-6.5	98.4	-9.5
GWS	0	0	0	0.5	0.3	94.2	-15.3	93.4	-14.8
TG	0	1	1	0	0.3	83.3	-3.4	80.6	-3.9

DOI: 10.1002/fld

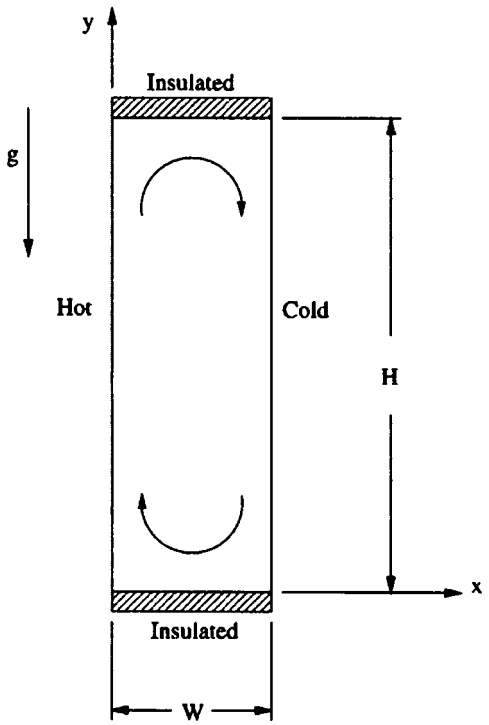

Figure 18. INS thermal cavity specification, 8×1 aspect ratio.

4.9. An incompressible Navier–Stokes validation

The final computational assessment of theory prediction of TWS-γ optimality is for a genuine INS validation problem. Selected is the 8×1 aspect ratio differentially heated natural convection cavity, Figure 18, for which experimental data confirm the resultant buoyancy-generated flowfields are Rayleigh number dependent. Specifically, these data confirm transition from a steady, single cell recirculation to an unsteady flowfield at a critical Rayleigh number [29]. Christon *et al.* [30] report the collection of CFD predictions of roughly two dozen numerical models, confirming that the critical Rayleigh number is $Ra_c \approx 3.1\text{E}{+}05$.

As computationally validated in [31], imposing $Ra > Ra_c$ generates an unsteady flowfield with significant multi-scale features induced by vortex-shedding vertical boundary layer separations yielding transient, multiple-scale circulating eddy distributions. This predicted multi-scale thermal flow field content is selected to evaluate the moderation of CFD algorithm GWS dispersion error *via* the TWS-γ algorithm.

The BCs for this problem statement are stationary with left and right wall temperatures constant at T_{hot} and T_{cold}, respectively, with the cavity top and bottom surfaces insulated. The gravitational body force operates vertically, which induces flowfield creation *via* natural convection. Thereby, it is appropriate to non-dimensionalize the INS system (5)–(7) using a reference velocity based on the thermal BC specification. Hence, define U_r as

$$U_r = \sqrt{\tau g \Delta T_r W} \tag{51}$$

DOI: 10.1002/fld

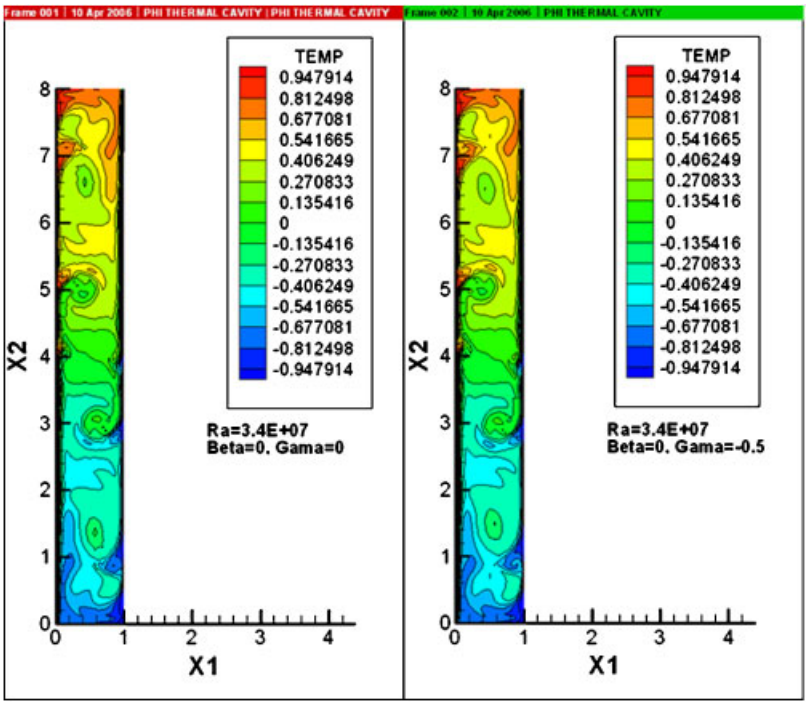

Figure 19. INS temperature distributions after 1500 time steps from the identical IC, GWS and TWS-γ algorithms, $Ra = 3.4\text{E}{+}07$, $M = 41 \times 201$.

where $\Delta T_r = T_{\text{hot}} - T_{\text{cold}}$ and W is the cavity width. This definition makes the Reynolds number proportional to the square root of Ra, defined as

$$Ra = \frac{g\tau \Delta T W^3}{Pr\text{Di}^2} \tag{52}$$

where Di is the thermal diffusivity. $Pr = 0.71$ is constant, and the computational test was conducted for $Ra = 3.4\text{E}{+}07$, well above the critical value. The associated Reynolds number is $Re = 6850$.

The required GWS and TWS-γ algorithms for the complete INS statement (5)–(10) exist in the UT CFD Lab research code *aPSE*. The theoretical formulation is due to Williams *et al.* [32] for imposing the constraint of continuity (5), which adds a pair of Poisson equations to the parent INS system. The TWS algorithm parameter definitions were $\alpha = 0 = \beta$, $\gamma = -0.5$ only for TWS-γ, and $\theta = 0.5$. The code implementation uses the FE bilinear basis for the entire state variable, and the mesh contained $M = 41 \times 201$ rectangular cartesian elements, solution-adapted *via* geometric progression refinement in all near-wall regions.

Figure 19 graphs the unsteady temperature distributions computed by the two considered algorithms, with IC a previously executed long-time solution, and integrating forward 1500 time steps at a fixed Δt. During these 1500 time steps, the unsteady flowfield 'turned over' in the cavity about twice. There exists a rich multi-scale distribution of thermal entities throughout the time evolution. The thermal boundary layers are very thin, corresponding to $Re = 6850$, and vortex

DOI: 10.1002/fld

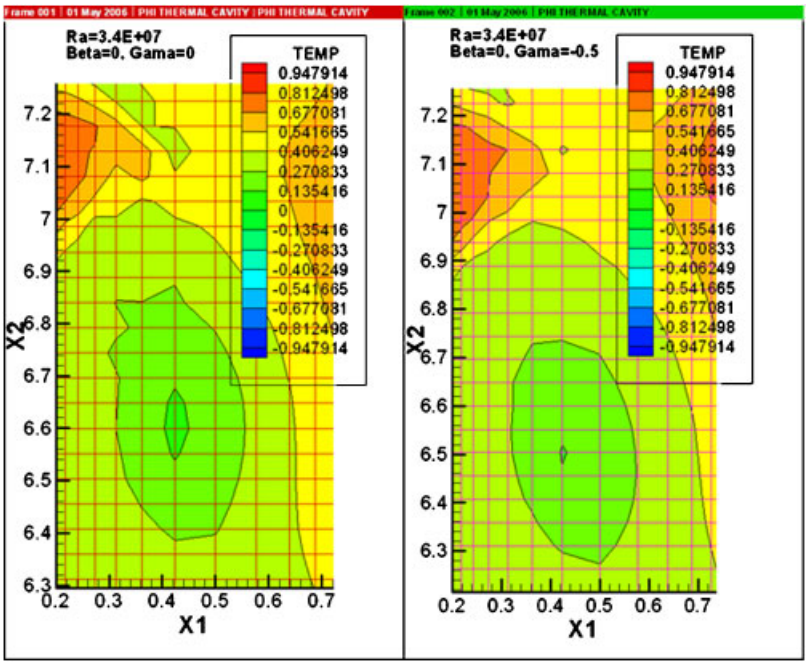

Figure 20. Close-up of INS temperature distributions after 1500 time steps for GWS and TWS-γ, $Ra = 3.4\text{E}{+}07$, $M = 41 \times 201$.

shedding from the vertical wall boundary layers is clearly visible about mid-height in the cavity at this time station.

On the scale of this presentation, the GWS and TWS-γ temperature solutions are visually very similar. However, windowing in on the significant thermal eddy structures about three-quarters up the left wall, the graphs in Figure 20 confirm that the GWS dispersion error-induced roughness of the temperature contours are significantly smoothed by the TWS-γ-algorithm. This observation can be quantified theoretically *via* the asymptotic error estimate (21). Specifically, the optimal solution will extremize the energy norm, and computational experience for thermal cavity problems, Ericson [33] confirms the approach is from below. The temperature energy norms for the GWS and TWS-γ solutions at this time station were 6.63116E$-$05 and 3.33277E$-$04 for $Ra = 3.4\text{E}{+}07$. A second simulation conducted at $Ra = 3.4\text{E}{+}08$ generated the corresponding norm comparison 2.086058E$-$07 and 2.086188E$-$07, respectively. These data pairs provide a sound mathematical confirmation of TWS-γ optimality.

Additional confirmation accrues to detailed *point norm* analysis of the velocity distribution at this time station. Figure 21 graphs the corresponding streamfunction distributions, as computed from the solution velocity vector fields *via* a weak statement on the calculus definition. In the *eyeball norm*, the inset close-ups of the vortex in the lower domain confirms the increased size of the bubble extremum for TWS-γ. Further, the TWS-γ solution exhibits streamfunction nodal extrema throughout the solution process. As detailed in Table V, at each time point in the unsteady evolution, the TWS-γ solution produces the extremum streamfunction range, which corresponds

DOI: 10.1002/fld

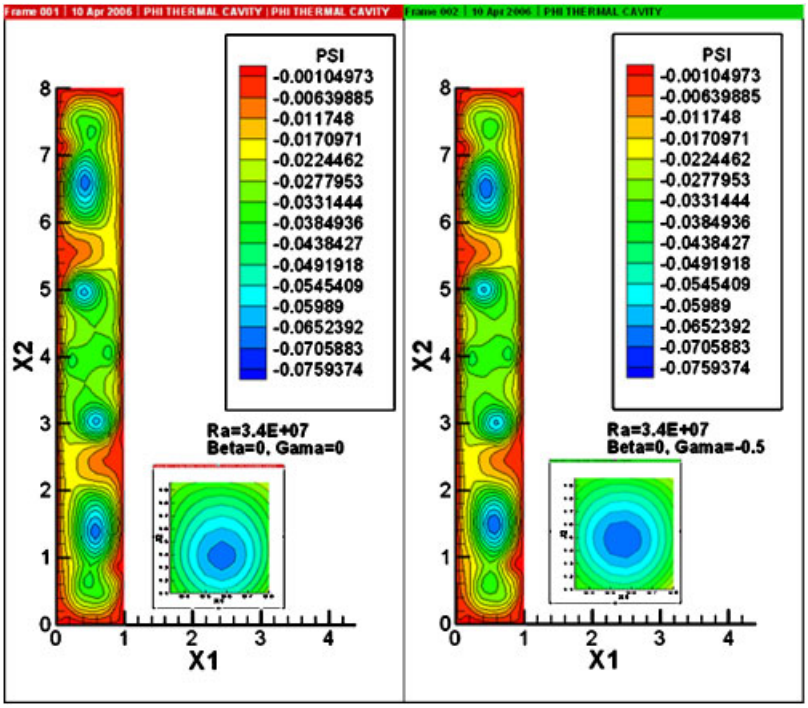

Figure 21. INS streamfunction distributions after 1500 time steps for GWS and TWS-γ, $Ra = 3.4\text{E}{+}07$, $M = 41 \times 201$.

Table V. INS 8×1 thermal cavity streamfunction extrema, $Ra = 3.4\text{E}{+}07$.

Time(s)		Min	Max
$Ra = 3.4\text{E}{+}07$, $Re = 6850$			
1.40E+02	$\gamma = 0$	−0.0795979	0.00114737
	$\gamma = -0.5$	−0.0795983	0.00114807
1.49E+02	$\gamma = 0$	−0.0808421	0.002806
	$\gamma = -0.5$	−0.0810310	0.003354
1.50E+02	$\gamma = 0$	−0.079579	0.0011473
	$\gamma = -0.5$	−0.079786	0.0018510
1.63E+02	$\gamma = 0$	−0.0687447	0.0004458
	$\gamma = -0.5$	−0.0704804	0.0012224

one to one with extremum velocity magnitude. These point norm data differences are indeed small, but in the right direction for every time station data pair, as required for further theory confirmation.

DOI: 10.1002/fld

5. CONCLUSIONS

The TWS^h + θTS algorithm spectral theory, developed in completeness for linear and bilinear FE basis implementations, provides a predictive framework for identifying optimal algorithm constructions in the class. The generated approximation error TS expansion in non-dimensional wave number space is precisely predictive of actual computational performance, as fully verified for the selected scalar transport test cases. The theory generated spectral distributions of phase velocity and amplification factor modulus error agree completely with the results of these tests. Finally, the theory contains as well the influence of time integration choice, the Courant vector magnitude and wave vector angle dependency, and further predicts angular quadrant independence.

The theory predicts, and test case results confirm, the superior performance of the TWS-γ algorithm over all other considered candidates in the class for 1D and 2D scalar advection. It is fair to assume this conclusion holds for 3D pure advection, and/or convection–diffusion as well. Anomalies in implementation of the theory were highlighted. Finally, computed results for a genuine unsteady incompressible-thermal NS validation-quality problem statement, containing significant multi-scale content for both vector and scalar fields, fully complements the required validation of the theory.

APPENDIX A: TS EXPANSION OF AMPLIFICATION FACTOR FOR TWS^h + θTS ALGORITHMS IN ORDERS OF NON-DIMENSIONAL WAVE NUMBER FOR 2D PURE ADVECTION

$$
\begin{aligned}
G^h = 1 &+ \frac{(-\mathrm{i}Ux\Delta t\Delta y^3\,\mathrm{Cos}[\eta] - \mathrm{i}Uy\Delta t\Delta y^3\,\mathrm{Sin}[\eta])m}{\Delta y^4} \\
&+ \left(-\frac{1}{\Delta y^4}\left(\frac{2}{27}Ux^2Uy^2\gamma^2\Delta t^4\,\mathrm{Cos}[\eta]^2 - \frac{1}{27}Uy^4\gamma^2\Delta t^4\,\mathrm{Cos}[\eta]^2 + \frac{4}{27}Ux^2\gamma\Delta t^2\Delta y^2\,\mathrm{Cos}[\eta]^2\right.\right. \\
&- \frac{4}{27}Uy^2\gamma\Delta t^2\Delta y^2\,\mathrm{Cos}[\eta]^2 - \frac{4}{27}\Delta y^4\,\mathrm{Cos}[\eta]^2 + Ux^2\Delta t^2\Delta y^2\theta^2\,\mathrm{Cos}[\eta]^2 \\
&+ 2UxUy\Delta t^2\Delta y^2\theta^2\,\mathrm{Cos}[\eta]\,\mathrm{Sin}[\eta] \\
&- \frac{1}{27}Ux^4\gamma^2\Delta t^4\,\mathrm{Sin}[\eta]^2 + \frac{2}{27}Ux^2Uy^2\gamma^2\Delta t^4\,\mathrm{Sin}[\eta]^2 - \frac{4}{27}Ux^2\gamma\Delta t^2\Delta y^2\,\mathrm{Sin}[\eta]^2 \\
&+ \frac{4}{27}Uy^2\gamma\Delta t^2\Delta y^2\,\mathrm{Sin}[\eta]^2 - \frac{4}{27}\Delta y^4\,\mathrm{Sin}[\eta]^2 + Uy^2\Delta t^2\Delta y^2\theta^2\,\mathrm{Sin}[\eta]^2 \\
&+ \frac{1}{81}Ux^4\gamma^2\Delta t^4(-\mathrm{Cos}[\eta]^2 - \mathrm{Sin}[\eta]^2) \\
&+ \frac{2}{81}Ux^2Uy^2\gamma^2\Delta t^4(-\mathrm{Cos}[\eta]^2 - \mathrm{Sin}[\eta]^2) + \frac{1}{81}Uy^4\gamma^2\Delta t^4(-\mathrm{Cos}[\eta]^2 - \mathrm{Sin}[\eta]^2) \\
&\left.\left. - \frac{2}{81}Ux^2\gamma\Delta t^2\Delta y^2(-\mathrm{Cos}[\eta]^2 - \mathrm{Sin}[\eta]^2) - \frac{2}{81}Uy^2\gamma\Delta t^2\Delta y^2(-\mathrm{Cos}[\eta]^2 - \mathrm{Sin}[\eta]^2)\right.\right.
\end{aligned}
$$

DOI: 10.1002/fld

$$
\begin{aligned}
&+\frac{1}{81}\Delta y^4(-\mathrm{Cos}[\eta]^2-\mathrm{Sin}[\eta]^2)-\frac{2}{81}Ux^4\gamma^2\Delta t^4\left(-\frac{1}{2}\,\mathrm{Cos}[\eta]^2-\mathrm{Sin}[\eta]^2\right)\\
&+\frac{2}{81}Ux^2Uy^2\gamma^2\Delta t^4\left(-\frac{1}{2}\,\mathrm{Cos}[\eta]^2-\mathrm{Sin}[\eta]^2\right)+\frac{4}{81}Uy^4\gamma^2\Delta t^4\left(-\frac{1}{2}\,\mathrm{Cos}[\eta]^2-\mathrm{Sin}[\eta]^2\right)\\
&-\frac{2}{81}Ux^2\gamma\Delta t^2\Delta y^2\left(-\frac{1}{2}\,\mathrm{Cos}[\eta]^2-\mathrm{Sin}[\eta]^2\right)-\frac{8}{81}Uy^2\gamma\Delta t^2\Delta y^2\left(-\frac{1}{2}\,\mathrm{Cos}[\eta]^2-\mathrm{Sin}[\eta]^2\right)\\
&+\frac{4}{81}\Delta y^4\left(-\frac{1}{2}\,\mathrm{Cos}[\eta]^2-\mathrm{Sin}[\eta]^2\right)+\frac{4}{81}Ux^4\gamma^2\Delta t^4\left(-\mathrm{Cos}[\eta]^2-\frac{\mathrm{Sin}[\eta]^2}{2}\right)\\
&+\frac{2}{81}Ux^2Uy^2\gamma^2\Delta t^4\left(-\mathrm{Cos}[\eta]^2-\frac{\mathrm{Sin}[\eta]^2}{2}\right)-\frac{2}{81}Uy^4\gamma^2\Delta t^4\left(-\mathrm{Cos}[\eta]^2-\frac{\mathrm{Sin}[\eta]^2}{2}\right)\\
&-\frac{8}{81}Ux^2\gamma\Delta t^2\Delta y^2\left(-\mathrm{Cos}[\eta]^2-\frac{\mathrm{Sin}[\eta]^2}{2}\right)-\frac{2}{81}Uy^2\gamma\Delta t^2\Delta y^2\left(-\mathrm{Cos}[\eta]^2-\frac{\mathrm{Sin}[\eta]^2}{2}\right)\\
&+\frac{4}{81}\Delta y^4\left(-\mathrm{Cos}[\eta]^2-\frac{\mathrm{Sin}[\eta]^2}{2}\right)-\frac{8}{81}Ux^4\gamma^2\Delta t^4\left(-\frac{1}{2}\mathrm{Cos}[\eta]^2-\frac{\mathrm{Sin}[\eta]^2}{2}\right)\\
&+\frac{2}{81}Ux^2Uy^2\gamma^2\Delta t^4\left(-\frac{1}{2}\mathrm{Cos}[\eta]^2-\frac{\mathrm{Sin}[\eta]^2}{2}\right)-\frac{8}{81}Uy^4\gamma^2\Delta t^4\left(-\frac{1}{2}\mathrm{Cos}[\eta]^2-\frac{\mathrm{Sin}[\eta]^2}{2}\right)\\
&-\frac{8}{81}Ux^2\gamma\Delta t^2\Delta y^2\left(-\frac{1}{2}\,\mathrm{Cos}[\eta]^2-\frac{\mathrm{Sin}[\eta]^2}{2}\right)-\frac{8}{81}Uy^2\gamma\Delta t^2\Delta y^2\left(-\frac{1}{2}\mathrm{Cos}[\eta]^2-\frac{\mathrm{Sin}[\eta]^2}{2}\right)\\
&+\frac{16}{81}\Delta y^4\left(-\frac{1}{2}\,\mathrm{Cos}[\eta]^2-\frac{\mathrm{Sin}[\eta]^2}{2}\right)\Bigg)\\
&+\frac{1}{\Delta y^4}\left(\frac{2}{27}Ux^2Uy^2\gamma^2\Delta t^4\,\mathrm{Cos}[\eta]^2-\frac{1}{27}Uy^4\gamma^2\Delta t^4\,\mathrm{Cos}[\eta]^2+\frac{4}{27}Ux^2\gamma\Delta t^2\Delta y^2\,\mathrm{Cos}[\eta]^2\right.\\
&-\frac{4}{27}Uy^2\gamma\Delta t^2\Delta y^2\,\mathrm{Cos}[\eta]^2-\frac{4}{27}\Delta y^4\,\mathrm{Cos}[\eta]^2-Ux^2\Delta t^2\Delta y^2\theta\,\mathrm{Cos}[\eta]^2\\
&+Ux^2\Delta t^2\Delta y^2\theta^2\,\mathrm{Cos}[\eta]^2\\
&-2UxUy\Delta t^2\Delta y^2\theta\,\mathrm{Cos}[\eta]\,\mathrm{Sin}[\eta]+2UxUy\Delta t^2\Delta y^2\theta^2\,\mathrm{Cos}[\eta]\,\mathrm{Sin}[\eta]-\frac{1}{27}Ux^4\gamma^2\Delta t^4\,\mathrm{Sin}[\eta]^2\\
&+\frac{2}{27}Ux^2Uy^2\gamma^2\Delta t^4\,\mathrm{Sin}[\eta]^2-\frac{4}{27}Ux^2\gamma\Delta t^2\Delta y^2\,\mathrm{Sin}[\eta]^2+\frac{4}{27}Uy^2\gamma\Delta t^2\Delta y^2\,\mathrm{Sin}[\eta]^2\\
&-\frac{4}{27}\Delta y^4\,\mathrm{Sin}[\eta]^2-Uy^2\Delta t^2\Delta y^2\theta\,\mathrm{Sin}[\eta]^2+Uy^2\Delta t^2\Delta y^2\theta^2\,\mathrm{Sin}[\eta]^2\\
&+\frac{1}{81}Ux^4\gamma^2\Delta t^4(-\mathrm{Cos}[\eta]^2-\mathrm{Sin}[\eta]^2)
\end{aligned}
$$

DOI: 10.1002/fld

$$
\begin{aligned}
&+\frac{2}{81}Ux^2Uy^2\gamma^2\Delta t^4(-\mathrm{Cos}[\eta]^2-\mathrm{Sin}[\eta]^2)+\frac{1}{81}Uy^4\gamma^2\Delta t^4(-\mathrm{Cos}[\eta]^2-\mathrm{Sin}[\eta]^2)\\
&-\frac{2}{81}Ux^2\gamma\Delta t^2\Delta y^2(-\mathrm{Cos}[\eta]^2-\mathrm{Sin}[\eta]^2)-\frac{2}{81}Uy^2\gamma\Delta t^2\Delta y^2(-\mathrm{Cos}[\eta]^2-\mathrm{Sin}[\eta]^2)\\
&+\frac{1}{81}\Delta y^4(-\mathrm{Cos}[\eta]^2-\mathrm{Sin}[\eta]^2)-\frac{2}{81}Ux^4\gamma^2\Delta t^4\left(-\frac{1}{2}\,\mathrm{Cos}[\eta]^2-\mathrm{Sin}[\eta]^2\right)\\
&+\frac{2}{81}Ux^2Uy^2\gamma^2\Delta t^4\left(-\frac{1}{2}\,\mathrm{Cos}[\eta]^2-\mathrm{Sin}[\eta]^2\right)+\frac{4}{81}Uy^4\gamma^2\Delta t^4\left(-\frac{1}{2}\,\mathrm{Cos}[\eta]^2-\mathrm{Sin}[\eta]^2\right)\\
&-\frac{2}{81}Ux^2\gamma\Delta t^2\Delta y^2\left(-\frac{1}{2}\,\mathrm{Cos}[\eta]^2-\mathrm{Sin}[\eta]^2\right)-\frac{8}{81}Uy^2\gamma\Delta t^2\Delta y^2\left(-\frac{1}{2}\,\mathrm{Cos}[\eta]^2-\mathrm{Sin}[\eta]^2\right)\\
&+\frac{4}{81}\Delta y^4\left(-\frac{1}{2}\,\mathrm{Cos}[\eta]^2-\mathrm{Sin}[\eta]^2\right)+\frac{4}{81}Ux^4\gamma^2\Delta t^4\left(-\mathrm{Cos}[\eta]^2-\frac{\mathrm{Sin}[\eta]^2}{2}\right)\\
&+\frac{2}{81}Ux^2Uy^2\gamma^2\Delta t^4\left(-\mathrm{Cos}[\eta]^2-\frac{\mathrm{Sin}[\eta]^2}{2}\right)-\frac{2}{81}Uy^4\gamma^2\Delta t^4\left(-\mathrm{Cos}[\eta]^2-\frac{\mathrm{Sin}[\eta]^2}{2}\right)\\
&-\frac{8}{81}Ux^2\gamma\Delta t^2\Delta y^2\left(-\mathrm{Cos}[\eta]^2-\frac{\mathrm{Sin}[\eta]^2}{2}\right)-\frac{2}{81}Uy^2\gamma\Delta t^2\Delta y^2\left(-\mathrm{Cos}[\eta]^2-\frac{\mathrm{Sin}[\eta]^2}{2}\right)\\
&+\frac{4}{81}\Delta y^4\left(-\mathrm{Cos}[\eta]^2-\frac{\mathrm{Sin}[\eta]^2}{2}\right)-\frac{8}{81}Ux^4\gamma^2\Delta t^4\left(-\frac{1}{2}\mathrm{Cos}[\eta]^2-\frac{\mathrm{Sin}[\eta]^2}{2}\right)\\
&+\frac{2}{81}Ux^2Uy^2\gamma^2\Delta t^4\left(-\frac{1}{2}\mathrm{Cos}[\eta]^2-\frac{\mathrm{Sin}[\eta]^2}{2}\right)-\frac{8}{81}Uy^4\gamma^2\Delta t^4\left(-\frac{1}{2}\mathrm{Cos}[\eta]^2-\frac{\mathrm{Sin}[\eta]^2}{2}\right)\\
&-\frac{8}{81}Ux^2\gamma\Delta t^2\Delta y^2\left(-\frac{1}{2}\,\mathrm{Cos}[\eta]^2-\frac{\mathrm{Sin}[\eta]^2}{2}\right)-\frac{8}{81}Uy^2\gamma\Delta t^2\Delta y^2\left(-\frac{1}{2}\mathrm{Cos}[\eta]^2-\frac{\mathrm{Sin}[\eta]^2}{2}\right)\\
&+\frac{16}{81}\Delta y^4\left(-\frac{1}{2}\,\mathrm{Cos}[\eta]^2-\frac{\mathrm{Sin}[\eta]^2}{2}\right)\Bigg)\Bigg)m^2\\
&+\Bigg(-\frac{1}{\Delta y^8}\Big((\mathrm{i}Ux\Delta t\Delta y^3\,\mathrm{Cos}[\eta]-\mathrm{i}Uy\Delta t\Delta y^3\,\mathrm{Sin}[\eta])\\
&\times\left(\frac{2}{27}Ux^2Uy^2\gamma^2\Delta t^4\,\mathrm{Cos}[\eta]^2-\frac{1}{27}Uy^4\gamma^2\Delta t^4\,\mathrm{Cos}[\eta]^2+\frac{4}{27}Ux^2\gamma\Delta t^2\Delta y^2\,\mathrm{Cos}[\eta]^2\right.\\
&-\frac{4}{27}Uy^2\gamma\Delta t^2\Delta y^2\,\mathrm{Cos}[\eta]^2-\frac{4}{27}\Delta y^4\,\mathrm{Cos}[\eta]^2+Ux^2\Delta t^2\Delta y^2\theta^2\,\mathrm{Cos}[\eta]^2\\
&+2UxUy\Delta t^2\Delta y^2\theta^2\,\mathrm{Cos}[\eta]\,\mathrm{Sin}[\eta]\\
&-\frac{1}{27}Ux^4\gamma^2\Delta t^4\,\mathrm{Sin}[\eta]^2+\frac{2}{27}Ux^2Uy^2\gamma^2\Delta t^4\,\mathrm{Sin}[\eta]^2-\frac{4}{27}Ux^2\gamma\Delta t^2\Delta y^2\,\mathrm{Sin}[\eta]^2
\end{aligned}
$$

DOI: 10.1002/fld

$$+\frac{4}{27}Uy^2\gamma\Delta t^2\Delta y^2\,\mathrm{Sin}[\eta]^2-\frac{4}{27}\Delta y^4\,\mathrm{Sin}[\eta]^2+Uy^2\Delta t^2\Delta y^2\theta^2\,\mathrm{Sin}[\eta]^2$$

$$+\frac{1}{81}Ux^4\gamma^2\Delta t^4(-\mathrm{Cos}[\eta]^2-\mathrm{Sin}[\eta]^2)+\frac{2}{81}Ux^2Uy^2\gamma^2\Delta t^4(-\mathrm{Cos}[\eta]^2-\mathrm{Sin}[\eta]^2)$$

$$+\frac{1}{81}Uy^4\gamma^2\Delta t^4(-\mathrm{Cos}[\eta]^2-\mathrm{Sin}[\eta]^2)-\frac{2}{81}Ux^2\gamma\Delta t^2\Delta y^2(-\mathrm{Cos}[\eta]^2-\mathrm{Sin}[\eta]^2)$$

$$-\frac{2}{81}Uy^2\gamma\Delta t^2\Delta y^2(-\mathrm{Cos}[\eta]^2-\mathrm{Sin}[\eta]^2)+\frac{1}{81}\Delta y^4(-\mathrm{Cos}[\eta]^2-\mathrm{Sin}[\eta]^2)$$

$$-\frac{2}{81}Ux^4\gamma^2\Delta t^4\left(-\frac{1}{2}\,\mathrm{Cos}[\eta]^2-\mathrm{Sin}[\eta]^2\right)+\frac{2}{81}Ux^2Uy^2\gamma^2\Delta t^4\left(-\frac{1}{2}\,\mathrm{Cos}[\eta]^2-\mathrm{Sin}[\eta]^2\right)$$

$$+\frac{4}{81}Uy^4\gamma^2\Delta t^4\left(-\frac{1}{2}\,\mathrm{Cos}[\eta]^2-\mathrm{Sin}[\eta]^2\right)-\frac{2}{81}Ux^2\gamma\Delta t^2\Delta y^2\left(-\frac{1}{2}\,\mathrm{Cos}[\eta]^2-\mathrm{Sin}[\eta]^2\right)$$

$$-\frac{8}{81}Uy^2\gamma\Delta t^2\Delta y^2\left(-\frac{1}{2}\,\mathrm{Cos}[\eta]^2-\mathrm{Sin}[\eta]^2\right)+\frac{4}{81}\Delta y^4\left(-\frac{1}{2}\,\mathrm{Cos}[\eta]^2-\mathrm{Sin}[\eta]^2\right)$$

$$+\frac{4}{81}Ux^4\gamma^2\Delta t^4\left(-\mathrm{Cos}[\eta]^2-\frac{\mathrm{Sin}[\eta]^2}{2}\right)+\frac{2}{81}Ux^2Uy^2\gamma^2\Delta t^4\left(-\mathrm{Cos}[\eta]^2-\frac{\mathrm{Sin}[\eta]^2}{2}\right)$$

$$-\frac{2}{81}Uy^4\gamma^2\Delta t^4\left(-\mathrm{Cos}[\eta]^2-\frac{\mathrm{Sin}[\eta]^2}{2}\right)-\frac{8}{81}Ux^2\gamma\Delta t^2\Delta y^2\left(-\mathrm{Cos}[\eta]^2-\frac{\mathrm{Sin}[\eta]^2}{2}\right)$$

$$-\frac{2}{81}Uy^2\gamma\Delta t^2\Delta y^2\left(-\mathrm{Cos}[\eta]^2-\frac{\mathrm{Sin}[\eta]^2}{2}\right)+\frac{4}{81}\Delta y^4\left(-\mathrm{Cos}[\eta]^2-\frac{\mathrm{Sin}[\eta]^2}{2}\right)$$

$$-\frac{8}{81}Ux^4\gamma^2\Delta t^4\left(-\frac{1}{2}\,\mathrm{Cos}[\eta]^2-\frac{\mathrm{Sin}[\eta]^2}{2}\right)+\frac{2}{81}Ux^2Uy^2\gamma^2\Delta t^4\left(-\frac{1}{2}\,\mathrm{Cos}[\eta]^2-\frac{\mathrm{Sin}[\eta]^2}{2}\right)$$

$$-\frac{8}{81}Uy^4\gamma^2\Delta t^4\left(-\frac{1}{2}\,\mathrm{Cos}[\eta]^2-\frac{\mathrm{Sin}[\eta]^2}{2}\right)-\frac{8}{81}Ux^2\gamma\Delta t^2\Delta y^2\left(-\frac{1}{2}\,\mathrm{Cos}[\eta]^2-\frac{\mathrm{Sin}[\eta]^2}{2}\right)$$

$$-\frac{8}{81}Uy^2\gamma\Delta t^2\Delta y^2\left(-\frac{1}{2}\,\mathrm{Cos}[\eta]^2-\frac{\mathrm{Sin}[\eta]^2}{2}\right)+\frac{16}{81}\Delta y^4\left(-\frac{1}{2}\,\mathrm{Cos}[\eta]^2-\frac{\mathrm{Sin}[\eta]^2}{2}\right)\Bigg)\Bigg)$$

$$+\frac{1}{\Delta y^4}\Bigg(-\frac{2}{27}\mathrm{i}Ux^3\gamma\Delta t^3\Delta y\,\mathrm{Cos}[\eta]^3+\frac{2}{27}\mathrm{i}UxUy^2\gamma\Delta t^3\Delta y\,\mathrm{Cos}[\eta]^3+\frac{4}{27}\mathrm{i}Ux\Delta t\Delta y^3\,\mathrm{Cos}[\eta]^3$$

$$+\frac{2}{27}\mathrm{i}Ux^3Uy\gamma\Delta t^3\Delta y\,\mathrm{Sin}[\eta]^3-\frac{2}{27}\mathrm{i}Uy^3\gamma\Delta t^3\Delta y\,\mathrm{Sin}[\eta]^3+\frac{4}{27}\mathrm{i}Uy\Delta t\Delta y^3\,\mathrm{Sin}[\eta]^3$$

$$-\frac{1}{27}\mathrm{i}Ux^3\gamma\Delta t^3\Delta y\left(-\frac{1}{6}\,\mathrm{Cos}[\eta]^3-\mathrm{Cos}[\eta]\,\mathrm{Sin}[\eta]^2\right)$$

$$+\frac{2}{27}\mathrm{i}UxUy^2\gamma\Delta t^3\Delta y\left(-\frac{1}{6}\,\mathrm{Cos}[\eta]^3-\mathrm{Cos}[\eta]\,\mathrm{Sin}[\eta]^2\right)$$

DOI: 10.1002/fld

$$
\begin{aligned}
&- \frac{2}{27}\mathrm{i}Ux\Delta t\Delta y^3\left(-\frac{1}{6}\,\mathrm{Cos}[\eta]^3 - \mathrm{Cos}[\eta]\,\mathrm{Sin}[\eta]^2\right)\\
&- \frac{4}{27}\mathrm{i}Ux^3\gamma\Delta t^3\Delta y\left(-\frac{1}{6}\,\mathrm{Cos}[\eta]^3 - \frac{1}{2}\,\mathrm{Cos}[\eta]\,\mathrm{Sin}[\eta]^2\right)\\
&+ \frac{2}{27}\mathrm{i}UxUy^2\gamma\Delta t^3\Delta y\left(-\frac{1}{6}\,\mathrm{Cos}[\eta]^3 - \frac{1}{2}\,\mathrm{Cos}[\eta]\,\mathrm{Sin}[\eta]^2\right)\\
&- \frac{8}{27}\mathrm{i}Ux\Delta t\Delta y^3\left(-\frac{1}{6}\,\mathrm{Cos}[\eta]^3 - \frac{1}{2}\,\mathrm{Cos}[\eta]\,\mathrm{Sin}[\eta]^2\right)\\
&+ \frac{2}{27}\mathrm{i}Ux^2Uy\gamma\Delta t^3\Delta y\left(-\mathrm{Cos}[\eta]^2\,\mathrm{Sin}[\eta] - \frac{\mathrm{Sin}[\eta]^3}{6}\right)\\
&- \frac{1}{27}\mathrm{i}Uy^3\gamma\Delta t^3\Delta y\left(-\mathrm{Cos}[\eta]^2\,\mathrm{Sin}[\eta] - \frac{\mathrm{Sin}[\eta]^3}{6}\right)\\
&- \frac{2}{27}\mathrm{i}Uy\Delta t\Delta y^3\left(-\mathrm{Cos}[\eta]^2\,\mathrm{Sin}[\eta] - \frac{\mathrm{Sin}[\eta]^3}{6}\right)\\
&+ \frac{2}{27}\mathrm{i}Ux^2Uy\gamma\Delta t^3\Delta y\left(-\frac{1}{2}\,\mathrm{Cos}[\eta]^2\,\mathrm{Sin}[\eta] - \frac{\mathrm{Sin}[\eta]^3}{6}\right)\\
&- \frac{4}{27}\mathrm{i}Uy^3\gamma\Delta t^3\Delta y\left(-\frac{1}{2}\,\mathrm{Cos}[\eta]^2\,\mathrm{Sin}[\eta] - \frac{\mathrm{Sin}[\eta]^3}{6}\right)\\
&- \frac{8}{27}\mathrm{i}Uy\Delta t\Delta y^3\left(-\frac{1}{2}\,\mathrm{Cos}[\eta]^2\,\mathrm{Sin}[\eta] - \frac{\mathrm{Sin}[\eta]^3}{6}\right)\\
&+ \frac{1}{27}\mathrm{i}Ux^3\gamma\Delta t^3\Delta y\left(-\frac{1}{6}\,\mathrm{Cos}[\eta]^3 + \mathrm{Cos}[\eta]\left(-\frac{1}{2}\,\mathrm{Cos}[\eta]^2 - \mathrm{Sin}[\eta]^2\right)\right)\\
&+ \frac{1}{27}\mathrm{i}UxUy^2\gamma\Delta t^3\Delta y\left(-\frac{1}{6}\,\mathrm{Cos}[\eta]^3 + \mathrm{Cos}[\eta]\left(-\frac{1}{2}\,\mathrm{Cos}[\eta]^2 - \mathrm{Sin}[\eta]^2\right)\right)\\
&- \frac{1}{27}\mathrm{i}Ux\Delta t\Delta y^3\left(-\frac{1}{6}\,\mathrm{Cos}[\eta]^3 + \mathrm{Cos}[\eta]\left(-\frac{1}{2}\,\mathrm{Cos}[\eta]^2 - \mathrm{Sin}[\eta]^2\right)\right)\\
&+ \frac{1}{27}\mathrm{i}Ux^2Uy\gamma\Delta t^3\Delta y\left(-\frac{1}{6}\,\mathrm{Sin}[\eta]^3 + \mathrm{Sin}[\eta]\left(-\mathrm{Cos}[\eta]^2 - \frac{\mathrm{Sin}[\eta]^2}{2}\right)\right)\\
&+ \frac{1}{27}\mathrm{i}Uy^3\gamma\Delta t^3\Delta y\left(-\frac{1}{6}\,\mathrm{Sin}[\eta]^3 + \mathrm{Sin}[\eta]\left(-\mathrm{Cos}[\eta]^2 - \frac{\mathrm{Sin}[\eta]^2}{2}\right)\right)\\
&- \frac{1}{27}\mathrm{i}Uy\Delta t\Delta y^3\left(-\frac{1}{6}\,\mathrm{Sin}[\eta]^3 + \mathrm{Sin}[\eta]\left(-\mathrm{Cos}[\eta]^2 - \frac{\mathrm{Sin}[\eta]^2}{2}\right)\right)
\end{aligned}
$$

DOI: 10.1002/fld

$$+\frac{4}{27}\mathrm{i}Ux^3\gamma\Delta t^3\Delta y\left(-\frac{1}{6}\mathrm{Cos}[\eta]^3+\mathrm{Cos}[\eta]\left(-\frac{1}{2}\mathrm{Cos}[\eta]^2-\frac{\mathrm{Sin}[\eta]^2}{2}\right)\right)$$

$$+\frac{1}{27}\mathrm{i}UxUy^2\gamma\Delta t^3\Delta y\left(-\frac{1}{6}\mathrm{Cos}[\eta]^3+\mathrm{Cos}[\eta]\left(-\frac{1}{2}\mathrm{Cos}[\eta]^2-\frac{\mathrm{Sin}[\eta]^2}{2}\right)\right)$$

$$-\frac{4}{27}\mathrm{i}Ux\Delta t\Delta y^3\left(-\frac{1}{6}\mathrm{Cos}[\eta]^3+\mathrm{Cos}[\eta]\left(-\frac{1}{2}\mathrm{Cos}[\eta]^2-\frac{\mathrm{Sin}[\eta]^2}{2}\right)\right)$$

$$+\frac{1}{27}\mathrm{i}Ux^2Uy\gamma\Delta t^3\Delta y\left(-\frac{1}{6}\mathrm{Sin}[\eta]^3+\mathrm{Sin}[\eta]\left(-\frac{1}{2}\mathrm{Cos}[\eta]^2-\frac{\mathrm{Sin}[\eta]^2}{2}\right)\right)$$

$$+\frac{4}{27}\mathrm{i}Uy^3\gamma\Delta t^3\Delta y\left(-\frac{1}{6}\mathrm{Sin}[\eta]^3+\mathrm{Sin}[\eta]\left(-\frac{1}{2}\mathrm{Cos}[\eta]^2-\frac{\mathrm{Sin}[\eta]^2}{2}\right)\right)$$

$$-\frac{4}{27}\mathrm{i}Uy\Delta t\Delta y^3\left(-\frac{1}{6}\mathrm{Sin}[\eta]^3+\mathrm{Sin}[\eta]\left(-\frac{1}{2}\mathrm{Cos}[\eta]^2-\frac{\mathrm{Sin}[\eta]^2}{2}\right)\right)\Bigg)\Bigg)\Bigg)m^3+O[m]^4$$

APPENDIX B: TS EXPANSION OF AMPLIFICATION FACTOR PHASE ERROR FOR TWS^h + θTS ALGORITHMS IN ORDERS OF NON-DIMENSIONAL WAVE NUMBER FOR 2D PURE ADVECTION

$$c^h_{k=1}=(\mathrm{i}Cx\,\mathrm{Cos}[\eta]-\mathrm{i}Ux\Delta t\,\mathrm{Cos}[\eta]+\mathrm{i}Cy\,\mathrm{Sin}[\eta]-\mathrm{i}Uy\Delta t\,\mathrm{Sin}[\eta])m$$

$$+(\mathrm{i}Cx\,\mathrm{Cos}[\eta]-\mathrm{i}Ux\Delta t\,\mathrm{Cos}[\eta]+\mathrm{i}Cy\,\mathrm{Sin}[\eta]-\mathrm{i}Uy\Delta t\,\mathrm{Sin}[\eta])m$$

$$+\Bigg(-\frac{1}{2}Ux^2\alpha\Delta t^2\,\mathrm{Cos}[\eta]^2-\frac{2}{9}Ux^2\beta\Delta t^2\,\mathrm{Cos}[\eta]^2$$

$$+\frac{2}{9}Uy^2\beta\Delta t^2\,\mathrm{Cos}[\eta]^2-\frac{2}{9}Ux^2Uy^2\beta\gamma\Delta t^4\,\mathrm{Cos}[\eta]^2+\frac{1}{9}Uy^4\beta\gamma\Delta t^4\,\mathrm{Cos}[\eta]^2$$

$$-Ux^2\Delta t^2\theta\,\mathrm{Cos}[\eta]^2-\frac{2}{3}Ux^2Uy^2\beta^2\Delta t^4\theta\,\mathrm{Cos}[\eta]^2+\frac{1}{3}Uy^4\beta^2\Delta t^4\theta\,\mathrm{Cos}[\eta]^2$$

$$-UxUy\alpha\Delta t^2\,\mathrm{Cos}[\eta]\,\mathrm{Sin}[\eta]-2UxUy\Delta t^2\theta\,\mathrm{Cos}[\eta]\,\mathrm{Sin}[\eta]-\frac{1}{2}Uy^2\alpha\Delta t^2\,\mathrm{Sin}[\eta]^2$$

$$+\frac{2}{9}Ux^2\beta\Delta t^2\,\mathrm{Sin}[\eta]^2-\frac{2}{9}Uy^2\beta\Delta t^2\,\mathrm{Sin}[\eta]^2+\frac{1}{9}Ux^4\beta\gamma\Delta t^4\,\mathrm{Sin}[\eta]^2$$

$$-\frac{2}{9}Ux^2Uy^2\beta\gamma\Delta t^4\,\mathrm{Sin}[\eta]^2-Uy^2\Delta t^2\theta\,\mathrm{Sin}[\eta]^2+\frac{1}{3}Ux^4\beta^2\Delta t^4\theta\,\mathrm{Sin}[\eta]^2$$

$$-\frac{2}{3}Ux^2Uy^2\beta^2\Delta t^4\theta\,\mathrm{Sin}[\eta]^2-\frac{1}{2}(-\mathrm{i}Cx\,\mathrm{Cos}[\eta]-\mathrm{i}Cy\,\mathrm{Sin}[\eta])^2$$

DOI: 10.1002/fld

$$
\begin{aligned}
&+\frac{1}{81}(-\mathrm{Cos}[\eta]^2-\mathrm{Sin}[\eta]^2)+\frac{1}{27}Ux^2\beta\Delta t^2(-\mathrm{Cos}[\eta]^2-\mathrm{Sin}[\eta]^2)\\
&+\frac{1}{27}Uy^2\beta\Delta t^2(-\mathrm{Cos}[\eta]^2-\mathrm{Sin}[\eta]^2)-\frac{2}{27}Ux^2Uy^2\beta\gamma\Delta t^4(-\mathrm{Cos}[\eta]^2-\mathrm{Sin}[\eta]^2)\\
&-\frac{2}{9}Ux^2Uy^2\beta^2\Delta t^4\theta(-\mathrm{Cos}[\eta]^2-\mathrm{Sin}[\eta]^2)+\frac{1}{27}Ux^2\beta\Delta t^2\left(-\frac{1}{2}\mathrm{Cos}[\eta]^2-\mathrm{Sin}[\eta]^2\right)\\
&+\frac{4}{27}Uy^2\beta\Delta t^2\left(-\frac{1}{2}\mathrm{Cos}[\eta]^2-\mathrm{Sin}[\eta]^2\right)+\frac{2}{27}Ux^4\beta\gamma\Delta t^4\left(-\frac{1}{2}\mathrm{Cos}[\eta]^2-\mathrm{Sin}[\eta]^2\right)\\
&+\frac{2}{27}Ux^2Uy^2\beta\gamma\Delta t^4\left(-\frac{1}{2}\mathrm{Cos}[\eta]^2-\mathrm{Sin}[\eta]^2\right)-\frac{4}{27}Uy^4\beta\gamma\Delta t^4\left(-\frac{1}{2}\mathrm{Cos}[\eta]^2-\mathrm{Sin}[\eta]^2\right)\\
&+\frac{2}{9}Ux^4\beta^2\Delta t^4\theta\left(-\frac{1}{2}\mathrm{Cos}[\eta]^2-\mathrm{Sin}[\eta]^2\right)-\frac{2}{9}Ux^2Uy^2\beta^2\Delta t^4\theta\left(-\frac{1}{2}\mathrm{Cos}[\eta]^2-\mathrm{Sin}[\eta]^2\right)\\
&-\frac{4}{9}Uy^4\beta^2\Delta t^4\theta\left(-\frac{1}{2}\mathrm{Cos}[\eta]^2-\mathrm{Sin}[\eta]^2\right)+\frac{4}{27}Ux^2\beta\Delta t^2\left(-\mathrm{Cos}[\eta]^2-\frac{\mathrm{Sin}[\eta]^2}{2}\right)\\
&+\frac{1}{27}Uy^2\beta\Delta t^2\left(-\mathrm{Cos}[\eta]^2-\frac{\mathrm{Sin}[\eta]^2}{2}\right)-\frac{4}{27}Ux^4\beta\gamma\Delta t^4\left(-\mathrm{Cos}[\eta]^2-\frac{\mathrm{Sin}[\eta]^2}{2}\right)\\
&-\frac{2}{27}Ux^2Uy^2\beta\gamma\Delta t^4\left(-\mathrm{Cos}[\eta]^2-\frac{\mathrm{Sin}[\eta]^2}{2}\right)+\frac{2}{27}Uy^4\beta\gamma\Delta t^4\left(-\mathrm{Cos}[\eta]^2-\frac{\mathrm{Sin}[\eta]^2}{2}\right)\\
&-\frac{4}{9}Ux^4\beta^2\Delta t^4\theta\left(-\mathrm{Cos}[\eta]^2-\frac{\mathrm{Sin}[\eta]^2}{2}\right)-\frac{2}{9}Ux^2Uy^2\beta^2\Delta t^2\theta\left(-\mathrm{Cos}[\eta]^2-\frac{\mathrm{Sin}[\eta]^2}{2}\right)\\
&+\frac{2}{9}Uy^4\beta^2\Delta t^4\theta\left(-\mathrm{Cos}[\eta]^2-\frac{\mathrm{Sin}[\eta]^2}{2}\right)+\frac{4}{27}Ux^2\beta\Delta t^2\left(-\frac{1}{2}\mathrm{Cos}[\eta]^2-\frac{\mathrm{Sin}[\eta]^2}{2}\right)\\
&+\frac{4}{27}Uy^2\beta\Delta t^2\left(-\frac{1}{2}\mathrm{Cos}[\eta]^2-\frac{\mathrm{Sin}[\eta]^2}{2}\right)+\frac{8}{27}Ux^4\beta\gamma\Delta t^4\left(-\frac{1}{2}\mathrm{Cos}[\eta]^2-\frac{\mathrm{Sin}[\eta]^2}{2}\right)\\
&-\frac{2}{27}Ux^2Uy^2\beta\gamma\Delta t^4\left(-\frac{1}{2}\mathrm{Cos}[\eta]^2-\frac{\mathrm{Sin}[\eta]^2}{2}\right)+\frac{8}{27}Uy^4\beta\gamma\Delta t^4\left(-\frac{1}{2}\mathrm{Cos}[\eta]^2-\frac{\mathrm{Sin}[\eta]^2}{2}\right)\\
&+\frac{8}{9}Ux^4\beta^2\Delta t^4\theta\left(-\frac{1}{2}\mathrm{Cos}[\eta]^2-\frac{\mathrm{Sin}[\eta]^2}{2}\right)-\frac{2}{9}Ux^2Uy^2\beta^2\Delta t^4\theta\left(-\frac{1}{2}\mathrm{Cos}[\eta]^2-\frac{\mathrm{Sin}[\eta]^2}{2}\right)\\
&+\frac{8}{9}Uy^4\beta^2\Delta t^4\theta\left(-\frac{1}{2}\mathrm{Cos}[\eta]^2-\frac{\mathrm{Sin}[\eta]^2}{2}\right)+\frac{1}{81}(\mathrm{Cos}[\eta]^2+\mathrm{Sin}[\eta]^2)\\
&+\frac{1}{27}Ux^4\beta\gamma\Delta t^4(\mathrm{Cos}[\eta]^2+\mathrm{Sin}[\eta]^2)+\frac{1}{27}Uy^4\beta\gamma\Delta t^4(\mathrm{Cos}[\eta]^2+\mathrm{Sin}[\eta]^2)
\end{aligned}
$$

DOI: 10.1002/fld

$$+\frac{1}{9}Ux^4\beta^2\Delta t^4\theta(\mathrm{Cos}[\eta]^2+\mathrm{Sin}[\eta]^2)+\frac{1}{9}Uy^4\beta^2\Delta t^4\theta(\mathrm{Cos}[\eta]^2+\mathrm{Sin}[\eta]^2)\Big)m^2$$

$$+\left(\frac{4}{27}\mathrm{i}Ux\Delta t\,\mathrm{Cos}[\eta]^3+\frac{1}{9}\mathrm{i}Ux^3\alpha\beta\Delta t^3\,\mathrm{Cos}[\eta]^3-\frac{1}{9}\mathrm{i}UxUy^2\alpha\beta\Delta t^3\,\mathrm{Cos}[\eta]^3\right.$$

$$+\frac{2}{27}\mathrm{i}Ux^3\gamma\Delta t^3\,\mathrm{Cos}[\eta]^3+\frac{2}{27}\mathrm{i}UxUy^2\gamma\Delta t^3\,\mathrm{Cos}[\eta]^3+\frac{4}{27}\mathrm{i}Uy\Delta t\,\mathrm{Sin}[\eta]^3$$

$$-\frac{1}{9}\mathrm{i}Ux^2Uy\alpha\beta\Delta t^3\,\mathrm{Sin}[\eta]^3+\frac{1}{9}\mathrm{i}Uy^3\alpha\beta\Delta t^3\,\mathrm{Sin}[\eta]^3$$

$$+\frac{2}{27}\mathrm{i}Ux^2Uy\gamma\Delta t^3\,\mathrm{Sin}[\eta]^3-\frac{2}{27}\mathrm{i}Uy^3\gamma\Delta t^3\,\mathrm{Sin}[\eta]^3$$

$$-\frac{1}{6}(-\mathrm{i}Cx\,\mathrm{Cos}[\eta]-\mathrm{i}Cy\,\mathrm{Sin}[\eta])^3-\frac{2}{27}\mathrm{i}Ux\Delta t\left(-\frac{1}{6}\mathrm{Cos}[\eta]^3-\mathrm{Cos}[\eta]\,\mathrm{Sin}[\eta]^2\right)$$

$$+\frac{1}{18}\mathrm{i}Ux^3\alpha\beta\Delta t^3\left(-\frac{1}{6}\mathrm{Cos}[\eta]^3-\mathrm{Cos}[\eta]\,\mathrm{Sin}[\eta]^2\right)$$

$$-\frac{1}{9}\mathrm{i}UxUy^2\alpha\beta\Delta t^3\left(-\frac{1}{6}\mathrm{Cos}[\eta]^3-\mathrm{Cos}[\eta]\,\mathrm{Sin}[\eta]^2\right)$$

$$-\frac{1}{27}\mathrm{i}Ux^3\gamma\Delta t^3\left(-\frac{1}{6}\mathrm{Cos}[\eta]^3-\mathrm{Cos}[\eta]\,\mathrm{Sin}[\eta]^2\right)$$

$$+\frac{2}{27}\mathrm{i}UxUy^2\gamma\Delta t^3\left(-\frac{1}{6}\mathrm{Cos}[\eta]^3-\mathrm{Cos}[\eta]\,\mathrm{Sin}[\eta]^2\right)$$

$$-\frac{8}{27}\mathrm{i}Ux\Delta t\left(-\frac{1}{6}\mathrm{Cos}[\eta]^3-\frac{1}{2}\mathrm{Cos}[\eta]\,\mathrm{Sin}[\eta]^2\right)$$

$$+\frac{2}{9}\mathrm{i}Ux^3\alpha\beta\Delta t^3\left(-\frac{1}{6}\mathrm{Cos}[\eta]^3-\frac{1}{2}\mathrm{Cos}[\eta]\,\mathrm{Sin}[\eta]^2\right)$$

$$-\frac{1}{9}\mathrm{i}UxUy^2\alpha\beta\Delta t^3\left(-\frac{1}{6}\mathrm{Cos}[\eta]^3-\frac{1}{2}\mathrm{Cos}[\eta]\,\mathrm{Sin}[\eta]^2\right)$$

$$-\frac{4}{27}\mathrm{i}Ux^3\gamma\Delta t^3\left(-\frac{1}{6}\mathrm{Cos}[\eta]^3-\frac{1}{2}\mathrm{Cos}[\eta]\,\mathrm{Sin}[\eta]^2\right)$$

$$+\frac{2}{27}\mathrm{i}UxUy^2\gamma\Delta t^3\left(-\frac{1}{6}\mathrm{Cos}[\eta]^3-\frac{1}{2}\mathrm{Cos}[\eta]\,\mathrm{Sin}[\eta]^2\right)$$

$$-\frac{2}{27}\mathrm{i}Uy\Delta t\left(-\mathrm{Cos}[\eta]^2\,\mathrm{Sin}[\eta]-\frac{\mathrm{Sin}[\eta]^3}{6}\right)$$

DOI: 10.1002/fld

$$
\begin{aligned}
&-\frac{1}{9}\mathrm{i}Ux^2Uy\alpha\beta\Delta t^3\left(-\mathrm{Cos}[\eta]^2\,\mathrm{Sin}[\eta]-\frac{\mathrm{Sin}[\eta]^3}{6}\right)\\
&+\frac{1}{18}\mathrm{i}Uy^3\alpha\beta\Delta t^3\left(-\mathrm{Cos}[\eta]^2\,\mathrm{Sin}[\eta]-\frac{\mathrm{Sin}[\eta]^3}{6}\right)\\
&+\frac{2}{27}\mathrm{i}Ux^2Uy\gamma\Delta t^3\left(-\mathrm{Cos}[\eta]^2\,\mathrm{Sin}[\eta]-\frac{\mathrm{Sin}[\eta]^3}{6}\right)-\frac{1}{27}\mathrm{i}Uy^3\gamma\Delta t^3\\
&\times\left(-\mathrm{Cos}[\eta]^2\,\mathrm{Sin}[\eta]-\frac{\mathrm{Sin}[\eta]^3}{6}\right)-\frac{8}{27}\mathrm{i}Uy\Delta t\left(-\frac{1}{2}\mathrm{Cos}[\eta]^2\,\mathrm{Sin}[\eta]-\frac{\mathrm{Sin}[\eta]^3}{6}\right)\\
&-\frac{1}{9}\mathrm{i}Ux^2Uy\alpha\beta\Delta t^3\left(-\frac{1}{2}\mathrm{Cos}[\eta]^2\,\mathrm{Sin}[\eta]-\frac{\mathrm{Sin}[\eta]^3}{6}\right)\\
&+\frac{2}{9}\mathrm{i}Uy^3\alpha\beta\Delta t^3\left(-\frac{1}{2}\mathrm{Cos}[\eta]^2\,\mathrm{Sin}[\eta]-\frac{\mathrm{Sin}[\eta]^3}{6}\right)\\
&+\frac{2}{27}\mathrm{i}Ux^2Uy\gamma\Delta t^3\left(-\frac{1}{2}\mathrm{Cos}[\eta]^2\,\mathrm{Sin}[\eta]-\frac{\mathrm{Sin}[\eta]^3}{6}\right)\\
&-\frac{4}{27}\mathrm{i}Uy^3\gamma\Delta t^3\left(-\frac{1}{2}\mathrm{Cos}[\eta]^2\,\mathrm{Sin}[\eta]-\frac{\mathrm{Sin}[\eta]^3}{6}\right)\\
&-\frac{1}{27}\mathrm{i}Ux\Delta t\left(-\frac{1}{6}\mathrm{Cos}[\eta]^3+\mathrm{Cos}[\eta]\left(-\frac{1}{2}\mathrm{Cos}[\eta]^2-\mathrm{Sin}[\eta]^2\right)\right)\\
&-\frac{1}{18}\mathrm{i}Ux^3\alpha\beta\Delta t^3\left(-\frac{1}{6}\mathrm{Cos}[\eta]^3+\mathrm{Cos}[\eta]\left(-\frac{1}{2}\mathrm{Cos}[\eta]^2-\mathrm{Sin}[\eta]^2\right)\right)\\
&-\frac{1}{18}\mathrm{i}UxUy^2\alpha\beta\Delta t^3\left(-\frac{1}{6}\mathrm{Cos}[\eta]^3+\mathrm{Cos}[\eta]\left(-\frac{1}{2}\mathrm{Cos}[\eta]^2-\mathrm{Sin}[\eta]^2\right)\right)\\
&+\frac{1}{27}\mathrm{i}Ux^3\gamma\Delta t^3\left(-\frac{1}{6}\mathrm{Cos}[\eta]^3+\mathrm{Cos}[\eta]\left(-\frac{1}{2}\mathrm{Cos}[\eta]^2-\mathrm{Sin}[\eta]^2\right)\right)\\
&+\frac{1}{27}\mathrm{i}UxUy^2\gamma\Delta t^3\left(-\frac{1}{6}\mathrm{Cos}[\eta]^3+\mathrm{Cos}[\eta]\left(-\frac{1}{2}\mathrm{Cos}[\eta]^2-\mathrm{Sin}[\eta]^2\right)\right)\\
&-\frac{1}{27}\mathrm{i}Uy\Delta t\left(-\frac{1}{6}\mathrm{Sin}[\eta]^3+\mathrm{Sin}[\eta]\left(-\mathrm{Cos}[\eta]^2-\frac{\mathrm{Sin}[\eta]^2}{2}\right)\right)\\
&-\frac{1}{18}\mathrm{i}Ux^2Uy\alpha\beta\Delta t^3\left(-\frac{1}{6}\mathrm{Sin}[\eta]^3+\mathrm{Sin}[\eta]\left(-\mathrm{Cos}[\eta]^2-\frac{\mathrm{Sin}[\eta]^2}{2}\right)\right)
\end{aligned}
$$

DOI: 10.1002/fld

$$
\begin{aligned}
&-\frac{1}{18}\mathrm{i}Uy^3\alpha\beta\Delta t^3\left(-\frac{1}{6}\mathrm{Sin}[\eta]^3+\mathrm{Sin}[\eta]\left(-\mathrm{Cos}[\eta]^2-\frac{\mathrm{Sin}[\eta]^2}{2}\right)\right)\\
&+\frac{1}{27}\mathrm{i}Ux^2Uy\gamma\Delta t^3\left(-\frac{1}{6}\mathrm{Sin}[\eta]^3+\mathrm{Sin}[\eta]\left(-\mathrm{Cos}[\eta]^2-\frac{\mathrm{Sin}[\eta]^2}{2}\right)\right)\\
&+\frac{1}{27}\mathrm{i}Uy^3\gamma\Delta t^3\left(-\frac{1}{6}\mathrm{Sin}[\eta]^3+\mathrm{Sin}[\eta]\left(-\mathrm{Cos}[\eta]^2-\frac{\mathrm{Sin}[\eta]^2}{2}\right)\right)\\
&-\frac{4}{27}\mathrm{i}Ux\Delta t\left(-\frac{1}{6}\mathrm{Cos}[\eta]^3+\mathrm{Cos}[\eta]\left(-\frac{1}{2}\mathrm{Cos}[\eta]^2-\frac{\mathrm{Sin}[\eta]^2}{2}\right)\right)\\
&-\frac{2}{9}\mathrm{i}Ux^3\alpha\beta\Delta t^3\left(-\frac{1}{6}\mathrm{Cos}[\eta]^3+\mathrm{Cos}[\eta]\left(-\frac{1}{2}\mathrm{Cos}[\eta]^2-\frac{\mathrm{Sin}[\eta]^2}{2}\right)\right)\\
&-\frac{1}{18}\mathrm{i}UxUy^2\alpha\beta\Delta t^3\left(-\frac{1}{6}\mathrm{Cos}[\eta]^3+\mathrm{Cos}[\eta]\left(-\frac{1}{2}\mathrm{Cos}[\eta]^2-\frac{\mathrm{Sin}[\eta]^2}{2}\right)\right)\\
&+\frac{4}{27}\mathrm{i}Ux^3\gamma\Delta t^3\left(-\frac{1}{6}\mathrm{Cos}[\eta]^3+\mathrm{Cos}[\eta]\left(-\frac{1}{2}\mathrm{Cos}[\eta]^2-\frac{\mathrm{Sin}[\eta]^2}{2}\right)\right)\\
&+\frac{1}{27}\mathrm{i}UxUy^2\gamma\Delta t^3\left(-\frac{1}{6}\mathrm{Cos}[\eta]^3+\mathrm{Cos}[\eta]\left(-\frac{1}{2}\mathrm{Cos}[\eta]^2-\frac{\mathrm{Sin}[\eta]^2}{2}\right)\right)\\
&-\frac{4}{27}\mathrm{i}Uy\Delta t\left(-\frac{1}{6}\mathrm{Sin}[\eta]^3+\mathrm{Sin}[\eta]\left(-\frac{1}{2}\mathrm{Cos}[\eta]^2-\frac{\mathrm{Sin}[\eta]^2}{2}\right)\right)\\
&-\frac{1}{18}\mathrm{i}Ux^2Uy\alpha\beta\Delta t^3\left(-\frac{1}{6}\mathrm{Sin}[\eta]^3+\mathrm{Sin}[\eta]\left(-\frac{1}{2}\mathrm{Cos}[\eta]^2-\frac{\mathrm{Sin}[\eta]^2}{2}\right)\right)\\
&-\frac{2}{9}\mathrm{i}Uy^3\alpha\beta\Delta t^3\left(-\frac{1}{6}\mathrm{Sin}[\eta]^3+\mathrm{Sin}[\eta]\left(-\frac{1}{2}\mathrm{Cos}[\eta]^2-\frac{\mathrm{Sin}[\eta]^2}{2}\right)\right)\\
&+\frac{1}{27}\mathrm{i}Ux^2Uy\gamma\Delta t^3\left(-\frac{1}{6}\mathrm{Sin}[\eta]^3+\mathrm{Sin}[\eta]\left(-\frac{1}{2}\mathrm{Cos}[\eta]^2-\frac{\mathrm{Sin}[\eta]^2}{2}\right)\right)\\
&+\frac{4}{27}\mathrm{i}Uy^3\gamma\Delta t^3\left(-\frac{1}{6}\mathrm{Sin}[\eta]^3+\mathrm{Sin}[\eta]\left(-\frac{1}{2}\mathrm{Cos}[\eta]^2-\frac{\mathrm{Sin}[\eta]^2}{2}\right)\right)\\
&+(-\mathrm{i}Ux\Delta t\,\mathrm{Cos}[\eta]-\mathrm{i}Uy\Delta t\,\mathrm{Sin}[\eta])\\
&\times\left(\frac{4\,\mathrm{Cos}[\eta]^2}{27}-\frac{1}{4}Ux^2\alpha^2\Delta t^2\,\mathrm{Cos}[\eta]^2-\frac{4}{27}Ux^2\gamma\Delta t^2\,\mathrm{Cos}[\eta]^2+\frac{4}{27}Uy^2\gamma\Delta t^2\,\mathrm{Cos}[\eta]^2\right.\\
&\left.-\frac{2}{27}Ux^2Uy^2\gamma^2\Delta t^4\,\mathrm{Cos}[\eta]^2+\frac{1}{27}Uy^4\gamma^2\Delta t^4\,\mathrm{Cos}[\eta]^2-Ux^2\alpha\Delta t^2\theta\,\mathrm{Cos}[\eta]^2\right.
\end{aligned}
$$

DOI: 10.1002/fld

$$
\begin{aligned}
&-\frac{4}{9}Ux^2\beta\Delta t^2\theta\,\mathrm{Cos}[\eta]^2+\frac{4}{9}Uy^2\beta\Delta t^2\theta\,\mathrm{Cos}[\eta]^2-\frac{4}{9}Ux^2Uy^2\beta\gamma\Delta t^4\theta\,\mathrm{Cos}[\eta]^2\\
&+\frac{2}{9}Uy^4\beta\gamma\Delta t^4\theta\,\mathrm{Cos}[\eta]^2-Ux^2\Delta t^2\theta^2\,\mathrm{Cos}[\eta]^2-\frac{2}{3}Ux^2Uy^2\beta^2\Delta t^4\theta^2\,\mathrm{Cos}[\eta]^2\\
&+\frac{1}{3}Uy^4\beta^2\Delta t^4\theta^2\,\mathrm{Cos}[\eta]^2-\frac{1}{2}UxUy\alpha^2\Delta t^2\,\mathrm{Cos}[\eta]\,\mathrm{Sin}[\eta]\\
&-2UxUy\alpha\Delta t^2\theta\,\mathrm{Cos}[\eta]\,\mathrm{Sin}[\eta]-2UxUy\Delta t^2\theta^2\,\mathrm{Cos}[\eta]\,\mathrm{Sin}[\eta]+\frac{4\,\mathrm{Sin}[\eta]^2}{27}\\
&-\frac{1}{4}Uy^2\alpha^2\Delta t^2\,\mathrm{Sin}[\eta]^2+\frac{4}{27}Ux^2\gamma\Delta t^2\,\mathrm{Sin}[\eta]^2-\frac{4}{27}Uy^2\gamma\Delta t^2\,\mathrm{Sin}[\eta]^2\\
&+\frac{1}{27}Ux^4\gamma^2\Delta t^4\,\mathrm{Sin}[\eta]^2-\frac{2}{27}Ux^2Uy^2\gamma^2\Delta t^4\,\mathrm{Sin}[\eta]^2-Uy^2\alpha\Delta t^2\theta\,\mathrm{Sin}[\eta]^2\\
&+\frac{4}{9}Ux^2\beta\Delta t^2\theta\,\mathrm{Sin}[\eta]^2-\frac{4}{9}Uy^2\beta\Delta t^2\theta\,\mathrm{Sin}[\eta]^2+\frac{2}{9}Ux^4\beta\gamma\Delta t^4\theta\,\mathrm{Sin}[\eta]^2\\
&-\frac{4}{9}Ux^2Uy^2\beta\gamma\Delta t^4\theta\,\mathrm{Sin}[\eta]^2-Uy^2\Delta t^2\theta^2\,\mathrm{Sin}[\eta]^2+\frac{1}{3}Ux^4\beta^2\Delta t^4\theta^2\,\mathrm{Sin}[\eta]^2\\
&-\frac{2}{3}Ux^2Uy^2\beta^2\Delta t^4\theta^2\,\mathrm{Sin}[\eta]^2+\frac{2}{81}Ux^2\gamma\Delta t^2(-\mathrm{Cos}[\eta]^2-\mathrm{Sin}[\eta]^2)\\
&+\frac{2}{81}Uy^2\gamma\Delta t^2(-\mathrm{Cos}[\eta]^2-\mathrm{Sin}[\eta]^2)-\frac{1}{81}Ux^4\gamma^2\Delta t^4(-\mathrm{Cos}[\eta]^2-\mathrm{Sin}[\eta]^2)\\
&-\frac{2}{81}Ux^2Uy^2\gamma^2\Delta t^4(-\mathrm{Cos}[\eta]^2-\mathrm{Sin}[\eta]^2)-\frac{1}{81}Uy^4\gamma^2\Delta t^4(-\mathrm{Cos}[\eta]^2-\mathrm{Sin}[\eta]^2)\\
&+\frac{2}{27}Ux^2\beta\Delta t^2\theta(-\mathrm{Cos}[\eta]^2-\mathrm{Sin}[\eta]^2)-\frac{2}{27}Uy^2\beta\Delta t^2\theta(-\mathrm{Cos}[\eta]^2-\mathrm{Sin}[\eta]^2)\\
&-\frac{2}{27}Ux^4\beta\gamma\Delta t^4\theta(-\mathrm{Cos}[\eta]^2-\mathrm{Sin}[\eta]^2)-\frac{4}{27}Ux^2Uy^2\beta\gamma\Delta t^4\theta(-\mathrm{Cos}[\eta]^2-\mathrm{Sin}[\eta]^2)\\
&-\frac{2}{27}Uy^4\beta\gamma\Delta t^4\theta(-\mathrm{Cos}[\eta]^2-\mathrm{Sin}[\eta]^2)-\frac{1}{9}Ux^4\beta^2\Delta t^4\theta^2(-\mathrm{Cos}[\eta]^2-\mathrm{Sin}[\eta]^2)\\
&-\frac{2}{9}Ux^2Uy^2\beta^2\Delta t^4\theta^2(-\mathrm{Cos}[\eta]^2-\mathrm{Sin}[\eta]^2)-\frac{1}{9}Uy^4\beta^2\Delta t^4\theta^2(-\mathrm{Cos}[\eta]^2-\mathrm{Sin}[\eta]^2)\\
&-\frac{4}{81}\left(-\frac{1}{2}\mathrm{Cos}[\eta]^2-\mathrm{Sin}[\eta]^2\right)+\frac{2}{81}Ux^2\gamma\Delta t^2\left(-\frac{1}{2}\mathrm{Cos}[\eta]^2-\mathrm{Sin}[\eta]^2\right)\\
&+\frac{8}{81}Uy^2\gamma\Delta t^2\left(-\frac{1}{2}\mathrm{Cos}[\eta]^2-\mathrm{Sin}[\eta]^2\right)+\frac{2}{81}Ux^4\gamma^2\Delta t^4\left(-\frac{1}{2}\mathrm{Cos}[\eta]^2-\mathrm{Sin}[\eta]^2\right)
\end{aligned}
$$

DOI: 10.1002/fld

$$
\begin{aligned}
&-\frac{2}{81}Ux^2Uy^2\gamma^2\Delta t^4\left(-\frac{1}{2}\mathrm{Cos}[\eta]^2-\mathrm{Sin}[\eta]^2\right)-\frac{4}{81}Uy^4\gamma^2\Delta t^4\left(-\frac{1}{2}\mathrm{Cos}[\eta]^2-\mathrm{Sin}[\eta]^2\right)\\
&+\left(-\frac{1}{2}\mathrm{Cos}[\eta]^2-\mathrm{Sin}[\eta]^2\right)+\frac{4}{81}Uy^4\gamma^2\Delta t^4\left(-\frac{1}{2}\mathrm{Cos}[\eta]^2-\mathrm{Sin}[\eta]^2\right)\\
&+\frac{2}{27}Ux^2\beta\Delta t^2\theta\left(-\frac{1}{2}\mathrm{Cos}[\eta]^2-\mathrm{Sin}[\eta]^2\right)+\frac{8}{27}Uy^2\beta\Delta t^2\theta\left(-\frac{1}{2}\mathrm{Cos}[\eta]^2-\mathrm{Sin}[\eta]^2\right)\\
&+\frac{4}{27}Ux^4\beta\gamma\Delta t^4\theta\left(-\frac{1}{2}\mathrm{Cos}[\eta]^2-\mathrm{Sin}[\eta]^2\right)-\frac{4}{27}Ux^2Uy^2\beta\gamma\Delta t^4\theta\left(-\frac{1}{2}\mathrm{Cos}[\eta]^2-\mathrm{Sin}[\eta]^2\right)\\
&-\frac{8}{27}Uy^4\beta\gamma\Delta t^4\theta\left(-\frac{1}{2}\mathrm{Cos}[\eta]^2-\mathrm{Sin}[\eta]^2\right)+\frac{2}{9}Ux^4\beta^2\Delta t^4\theta^2\left(-\frac{1}{2}\mathrm{Cos}[\eta]^2-\mathrm{Sin}[\eta]^2\right)\\
&-\frac{2}{9}Ux^2Uy^2\beta^2\Delta t^4\theta^2\left(-\frac{1}{2}\mathrm{Cos}[\eta]^2-\mathrm{Sin}[\eta]^2\right)\\
&-\frac{4}{9}Uy^4\beta^2\Delta t^4\theta^2\left(-\frac{1}{2}\mathrm{Cos}[\eta]^2-\mathrm{Sin}[\eta]^2\right)-\frac{4}{81}\left(-\mathrm{Cos}[\eta]^2-\frac{\mathrm{Sin}[\eta]^2}{2}\right)\\
&+\frac{8}{81}Ux^2\gamma\Delta t^2\left(-\mathrm{Cos}[\eta]^2-\frac{\mathrm{Sin}[\eta]^2}{2}\right)-\frac{2}{81}Uy^2\gamma\Delta t^2\left(-\mathrm{Cos}[\eta]^2-\frac{\mathrm{Sin}[\eta]^2}{2}\right)\\
&-\frac{4}{81}Ux^4\gamma\Delta t^4\left(-\mathrm{Cos}[\eta]^2-\frac{\mathrm{Sin}[\eta]^2}{2}\right)-\frac{2}{81}Ux^2Uy^2\gamma^2\Delta t^4\left(-\mathrm{Cos}[\eta]^2-\frac{\mathrm{Sin}[\eta]^2}{2}\right)\\
&+\frac{2}{81}Uy^4\gamma^2\Delta t^4\left(-\mathrm{Cos}[\eta]^2-\frac{\mathrm{Sin}[\eta]^2}{2}\right)+\frac{8}{27}Ux^2\beta\Delta t^2\theta\left(-\mathrm{Cos}[\eta]^2-\frac{\mathrm{Sin}[\eta]^2}{2}\right)\\
&+\frac{2}{27}Uy^2\beta\Delta t^2\theta\left(-\mathrm{Cos}[\eta]^2-\frac{\mathrm{Sin}[\eta]^2}{2}\right)-\frac{8}{27}Ux^4\beta\gamma\Delta t^4\theta\left(-\mathrm{Cos}[\eta]^2-\frac{\mathrm{Sin}[\eta]^2}{2}\right)\\
&-\frac{4}{27}Ux^2Uy^2\beta\gamma\Delta t^4\theta\left(-\mathrm{Cos}[\eta]^2-\frac{\mathrm{Sin}[\eta]^2}{2}\right)\\
&+\frac{4}{27}Uy^4\beta\gamma\Delta t^4\theta\left(-\mathrm{Cos}[\eta]^2-\frac{\mathrm{Sin}[\eta]^2}{2}\right)-\frac{4}{9}Ux^4\beta^2\Delta t^4\theta^2\left(-\mathrm{Cos}[\eta]^2-\frac{\mathrm{Sin}[\eta]^2}{2}\right)\\
&-\frac{2}{9}Ux^2Uy^2\beta^2\Delta t^4\theta^2\left(-\mathrm{Cos}[\eta]^2-\frac{\mathrm{Sin}[\eta]^2}{2}\right)+\frac{2}{9}Uy^4\beta^2\Delta t^4\theta^2\left(-\mathrm{Cos}[\eta]^2-\frac{\mathrm{Sin}[\eta]^2}{2}\right)\\
&-\frac{16}{81}\left(-\frac{1}{2}\mathrm{Cos}[\eta]^2-\frac{\mathrm{Sin}[\eta]^2}{2}\right)-\frac{8}{81}Ux^2\gamma\Delta t^2\left(-\frac{1}{2}\mathrm{Cos}[\eta]^2-\frac{\mathrm{Sin}[\eta]^2}{2}\right)
\end{aligned}
$$

DOI: 10.1002/fld

$$+\frac{8}{81}Uy^2\gamma\Delta t^2\left(-\frac{1}{2}\mathrm{Cos}[\eta]^2-\frac{\mathrm{Sin}[\eta]^2}{2}\right)+\frac{8}{81}Ux^4\gamma^2\Delta t^4\left(-\frac{1}{2}\mathrm{Cos}[\eta]^2-\frac{\mathrm{Sin}[\eta]^2}{2}\right)$$

$$-\frac{2}{81}Ux^2Uy^2\gamma^2\Delta t^4\left(-\frac{1}{2}\mathrm{Cos}[\eta]^2-\frac{\mathrm{Sin}[\eta]^2}{2}\right)$$

$$+\frac{8}{81}Uy^4\gamma^2\Delta t^4\left(-\frac{1}{2}\mathrm{Cos}[\eta]^2-\frac{\mathrm{Sin}[\eta]^2}{2}\right)+\frac{8}{27}Ux^2\beta\Delta t^2\theta\left(-\frac{1}{2}\mathrm{Cos}[\eta]^2-\frac{\mathrm{Sin}[\eta]^2}{2}\right)$$

$$+\frac{8}{27}Uy^2\beta\Delta t^2\theta\left(-\frac{1}{2}\mathrm{Cos}[\eta]^2-\frac{\mathrm{Sin}[\eta]^2}{2}\right)+\frac{16}{27}Ux^4\beta\Delta t^4\theta\left(-\frac{1}{2}\mathrm{Cos}[\eta]^2-\frac{\mathrm{Sin}[\eta]^2}{2}\right)$$

$$-\frac{4}{27}Ux^2Uy^2\beta\gamma\Delta t^4\theta\left(-\frac{1}{2}\mathrm{Cos}[\eta]^2-\frac{\mathrm{Sin}[\eta]^2}{2}\right)$$

$$+\frac{16}{27}Uy^4\beta\gamma\Delta t^4\theta\left(-\frac{1}{2}\mathrm{Cos}[\eta]^2-\frac{\mathrm{Sin}[\eta]^2}{2}\right)+\frac{8}{9}Ux^4\beta^2\Delta t^4\theta^2$$

$$\times\left(-\frac{1}{2}\mathrm{Cos}[\eta]^2-\frac{\mathrm{Sin}[\eta]^2}{2}\right)-\frac{2}{9}Ux^2Uy^2\beta^2\Delta t^4\theta^2\left(-\frac{1}{2}\mathrm{Cos}[\eta]^2-\frac{\mathrm{Sin}[\eta]^2}{2}\right)$$

$$+\frac{8}{9}Uy^4\beta^2\Delta t^4\theta^2\left(-\frac{1}{2}\mathrm{Cos}[\eta]^2-\frac{\mathrm{Sin}[\eta]^2}{2}\right)+\frac{1}{81}(\mathrm{Cos}[\eta]^2+\mathrm{Sin}[\eta]^2)\Bigg)m^3+O[m]^4$$

ACKNOWLEDGEMENTS

This work forms a portion of the PhD dissertation project of the first author, who wishes to acknowledge the GRA support provided by NSF, under grant DUE 0121669, also that provided by ARC Automotive, Inc. All computations were performed in the UT CFD Laboratory Beowulf PC computer complex.

REFERENCES

1. Belytschko T, Mullen R. On dispersive properties of finite element solutions. In *Modern Problems in Elastic Wave Propagation*, Milovitz J, Achenbach JD (eds). Wiley: New York, 1978; 67–82.
2. Vichnevetsky R, Bowles JB. *Fourier Analysis of Numerical Approximations of Hyperbolic Problems*. SIAM: Philadelphia, PA, 1982.
3. Vichnevetsky R. Wave propagation analysis of difference schemes for hyperbolic equations: a review. *International Journal for Numerical Methods in Fluids* 1987; **7**:409–452.
4. Shakib F, Hughes TJR. A new finite element formulation for computational fluid dynamics: IX Fourier analysis of space–time Galerkin/least-squares algorithms. *Computer Methods in Applied Mechanics and Engineering* 1991; **87**:35–58.
5. Morton KW, Mayers DF. *Numerical Solution of Partial Differential Equations*. Cambridge University Press: Cambridge, England, 1994.
6. Christon MA. The influence of the mass matrix on the dispersive nature of the semi-discrete, second-order wave equation. *Computer Methods in Applied Mechanics and Engineering* 1999; **173**:147–166.

DOI: 10.1002/fld

7. Christon MA, Martinez MJ, Voth TE. Generalized Fourier analyses of the advection–diffusion equation—part I: one-dimensional domains. *International Journal for Numerical Methods in Fluids* 2004; **45**:839–887.
8. Voth TE, Martinez MJ, Christon MA. Generalized Fourier analyses of the advection–diffusion equation—part II: two-dimensional domains. *International Journal for Numerical Methods in Fluids* 2004; **45**:889–920.
9. Oden JT, Reddy JN. *An Introduction to the Mathematical Theory of Finite Elements*. Wiley: New York, 1976.
10. Oden JT, Demkowicz LF. *Applied Functional Analysis*. CRC Press: Boca Raton, FL, 1996.
11. Wahlbin LB. A dissipative Galerkin method applied to some quasi-linear hyperbolic equations. *RAIRO* 1974; **8**:109–117.
12. Dendy JE. Two methods of Galerkin type achieving optimum L^2 rates of convergence for first-order hyperbolics. *SIAM Journal on Numerical Analysis* 1974; **11**:637–653.
13. Raymond WH, Garder A. Selective damping in a Galerkin method for solving wave problems with variable grids. *Monthly Weather Review* 1976; **104**:1583–1591.
14. Donea J. A Taylor–Galerkin algorithm for hyperbolic conservation laws. *International Journal for Numerical Methods in Engineering* 1984; **20**:101–119.
15. Brooks A, Hughes TJR. Streamline upwind/Petrov–Galerkin formulations for convection dominated flows with particular emphasis on the incompressible Navier–Stokes equations. *Computer Methods in Applied Mechanics and Engineering* 1982; **32**:199–259.
16. Jiang B. *The Least-Squares Finite Element Method*. Springer: Heidelberg, 1998.
17. Baker AJ, Kim JW. A Taylor weak statement for hyperbolic conservation laws. *International Journal for Numerical Methods in Fluids* 1987; **7**:489–520.
18. Chaffin DJ, Baker AJ. On Taylor weak statement finite element methods for computational fluid dynamics. *International Journal for Numerical Methods in Fluids* 1995; **21**:273–294.
19. Kolesnikov A, Baker AJ. An efficient high order Taylor weak statement formulation for the Navier–Stokes equations. *Journal of Computational Physics* 2001; **173**:549–574.
20. Li BQ. *Discontinuous Finite Elements in Fluid Dynamics and Heat Transfer*. Springer: New York, 2006.
21. Gresho PM, Sani RL. *Incompressible Flow and the Finite Element Method*, vol. I. Wiley: Chichester, England, 2000.
22. Haberman R. *Elementary Applied Partial Differential Equations* (3rd edn). Prentice-Hall: Englewood Cliffs, NJ, 1998.
23. Incropera FP, Dewitt DP. *Fundamentals of Heat and Mass Transfer* (5th edn). Wiley: New York, 2002.
24. Baker AJ. *The Computational Engineering Sciences*. j-Computek Press: Loudon, TN, 2006.
25. Crank J, Nicolson P. A practical method for numerical evaluation of solutions of partial differential equations of the heat conduction type. *Advances in Computational Mathematics* 1996; **6**(1):207–226.
26. Sahu S. A theory for modified conservation principles optimization of CFD algorithm fidelity. *Ph.D. Dissertation*, University of Tennessee, Knoxville, TN, 2006.
27. Trabia MB, Lu XB. A fuzzy adaptive simplex search optimization algorithm. *Journal of Mechanical Design* 2001; **123**:216–225.
28. Baker AJ. *Finite Element Computational Fluid Mechanics*. Taylor and Francis: Washington, DC, 1983.
29. Quere LP. Onset of unsteadiness, routes to chaos and simulations of chaotic flows in cavities heated from the side: a review of present status. *Proceedings of the 10th International Heat Transfer Conference*, Brighton, U.K., 1994; 281–296.
30. Christon M, Gresho PM, Sutton SB. Computational predictability of time-dependent natural convection flows in enclosures. *International Journal for Numerical Methods in Fluids* 2002; **40**:953–980.
31. Grubert M. Development of a potentially accurate and efficient LES CFD algorithm to predict heat and mass transport in inhabited spaces. *Ph.D. Dissertation*, University of Tennessee, Knoxville, TN, 2006.
32. Williams PT, Baker AJ. Incompressible computational fluid dynamics and the continuity constraint method for the 3-D Navier–Stokes equations. *Journal of Numerical Heat Transfer*, *Part B—Fundamentals* 1996; **29**:137–273.
33. Ericson SC. A CFD Laboratory archive supporting the academic process. *M.Sc. Thesis*, University of Tennessee, Knoxville, TN, 2001.

DOI: 10.1002/fld